GOCE-GDC: Towards a better understanding of the Earth's interior and geophysical exploration research Work Package 5 - Geophysics B

Zdeněk Martinec

Dublin Institute for Advanced Studies
5 Merrion Square, Dublin 2, Ireland

(i) GOCE solid Earth workshop (October 16-17, 2012)
(ii) Joint science meeting GOCE+ GeoExplore and GOCE+ GDC (October 18)
(iii) GOCE+ GDC MTR (October 19)

University of Twente, Enschede

Contents

What can we learn from the geoid on the solid Earth?

Newton's law of gravity:

$$V(P) = G \int_B \frac{\varrho(Q)}{d_{PQ}} \, dV_Q$$

- The **inverse gravimetric problem (IGP)**:
  Find the volume-mass distribution ϱ of the Earth, provided that the potential V is known outside the Earth.
- An inverse problem is called **well-posed** if each of the following three criteria is satisfied (Hadamard):
  - a solution exists
  - the solution is unique
  - the solution is stable, i.e. it continuously depends on the given data (here: V)

Inverse gravimetric problem is ill-posed

The IGP is an **ill-posed** inverse problem since violates all three of Hadamard's criteria.

- **Existence**: V has to be harmonic outside the Earth which may be violated by measurement erros
- **Uniqueness**: Only the harmonic part of the density function can uniquely be reconstructed, whereas the (in the sense of the L2-space) orthogonal, so-called anharmonic, part has the external potential 0 and, therefore, does not leave any trace in gravitational measurements. This is the most serious problem of IGP.
- **Stability**: The density does not continuously depend on the gravitational potential.

Non-uniqueness

Let ϱ_1 be a solution of the IGP and let ∂B have a continuous normal **n**.
Then a class of all solutions of the IGP in $L^2(B)$ can be represented as

$$\varrho = \varrho_1 + \nabla^2 h$$

where

$$h|_{\partial B} = \left.\frac{\partial h}{\partial n}\right|_{\partial B} = 0$$

In other words, $\nabla^2 h$ generates a **null** external gravitational field.
The Green's third identity proves this: for P in $E_3 \setminus B$ it holds

$$V(P) = G\int_B \frac{\nabla^2 h(Q)}{d_{PQ}}\, dV_Q = G\int_{\partial B}\left[\frac{\partial h(Q)}{\partial n}\frac{1}{d_{PQ}} - h(Q)\frac{\partial}{\partial n}\left(\frac{1}{d_{PQ}}\right)\right] dS_Q = 0$$

i.e., $V = 0$ in $E_3 \setminus B$ and hence on ∂B.

Minimum-norm solution

The minimum-norm solution:

$$\int_B [\delta\varrho(r,\Omega)]^2 \, dV = \min_{\delta\varrho}$$

under the integral constraints for potential coefficients

$$V_{jm} = \int_B \delta\varrho(r,\Omega) r^j Y_{jm}(\Omega) dV$$

The variational form using the Lagrange-multiplier method

$$\delta \left\{ \frac{1}{2} \int_B [\delta\varrho(r,\Omega)]^2 \, dV + \sum_{j=0}^{j_{max}} \sum_{m=-j}^{j} \alpha_{jm} \left[V_{jm} - \int_B \delta\varrho(r,\Omega) r^j Y_{jm}(\Omega) dV \right] \right\} = 0$$

where δ is the variation with respect to $\delta\varrho$.

$\Rightarrow$ **harmonic density anomaly**

$$\delta\varrho(r,\Omega) = \sum_{j=0}^{j_{max}} \sum_{m=-j}^{j} \alpha_{jm} r^j Y_{jm}(\Omega)$$

The decomposition of L_2 space

$$L_2 = H \oplus H^{\perp}$$

$$H := \left\{ r^j Y_{jm}(\Omega),\ j = 0, 1, \ldots, m = -j, \ldots, j \right\}$$

$$H^{\perp} := \left\{ \nabla^2 h,\ h|_{\partial B} = \left. \frac{\partial h}{\partial n} \right|_{\partial B} = 0 \right\}$$

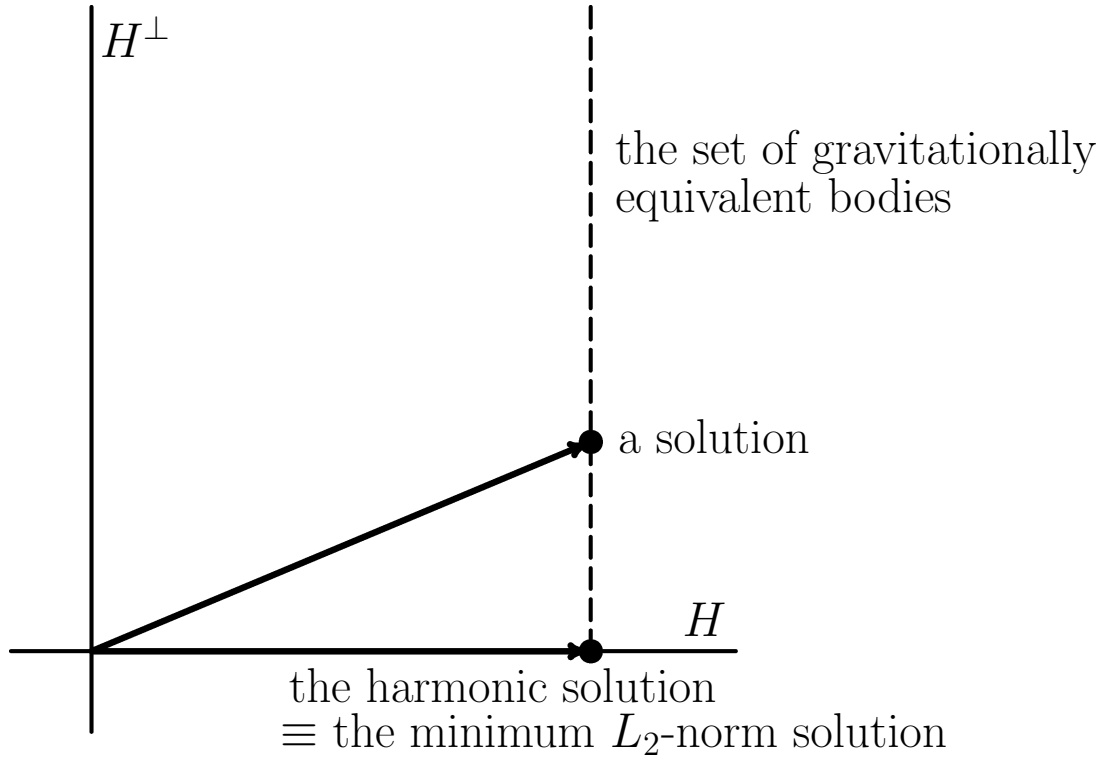

Instability

Let $\sigma = 0$ on ∂B and let $\varrho := 0$ in $E_3 \backslash B$. The Laplace-Poisson equation for potential V:

$$\nabla^2 V = -4\pi G\varrho \qquad \text{in } E_3$$

Using the 3-D Fourier transform of the form

$$\widetilde{f}(\mathbf{k}) = (2\pi)^{-3/2} \int_{E_3} f(\mathbf{r})\, e^{-i\mathbf{k}.\mathbf{r}}\, d^3\mathbf{r}$$

The Laplace-Poisson equation in the Fourier domain:

$$k^2 \widetilde{V}(\mathbf{k}) = 4\pi G\widetilde{\varrho}(\mathbf{k}) \qquad k = |\mathbf{k}|$$

Two possible views:

Forward GP

$$\widetilde{V}(\mathbf{k}) = A(\mathbf{k})\widetilde{\varrho}(\mathbf{k})$$

Inverse GP

$$\widetilde{\varrho}(\mathbf{k}) = \widetilde{V}(\mathbf{k})/A(\mathbf{k})$$

The **transfer function** mapping the density ϱ onto the potential V:

$$\boxed{A(\mathbf{k}) = \frac{4\pi G}{k^2}}$$

For $k \to \infty$, $1/A(\mathbf{k}) \to \infty$, and a solution of the IGP is **unstable**.

Do gradiometric data bring new information on mass density?

Answer: **NO** if the gradiometric data are considered as the Stokes potential coefficients

Spherical harmonic representation of V

$$V(r,\Omega) = \frac{GM}{a}\sum_{j=0}^{\infty}\left(\frac{a}{r}\right)^{j+1}\sum_{m=-j}^{j} V_{jm}\,Y_{jm}(\Omega)$$

Stokes potential coefficients

$$V_{jm} = \frac{4\pi}{Ma^j}\frac{1}{2j+1}\int_{\mathcal{B}} r'^j\,\varrho(r',\Omega')\,Y^*_{jm}(\Omega')\,dV'$$

Gradiometric model (e.g. GOCO02)

$$\text{grad grad}\,V(r,\Omega) = GM\sum_{j=0}^{\infty}a^j\sum_{m=-j}^{j}V_{jm}^{\text{GOCE}}\,\text{grad grad}\left[r^{-j-1}\,Y_{jm}(\Omega)\right]$$

Green's function of geoid for a static mantle

Newton's integral:

$$\delta V(r,\Omega) = G\int_{r'=b}^{a}\int_{\Omega_0}\frac{\delta\varrho(r',\Omega')}{L(r,\psi,r')}r'^2 dr' d\Omega'$$

Using the addition theorem for $r > r'$,

$$\frac{1}{L(r,\psi,r')} = \frac{4\pi}{r}\sum_{j=0}^{\infty}\sum_{m=-j}^{j}\frac{1}{2j+1}\left(\frac{r'}{r}\right)^j Y_{jm}^*(\Omega')\,Y_{jm}(\Omega)\ ,$$

and writing the spherical harmonic expansions:

$$\delta V(r,\Omega) = \sum_{jm}\delta V_{jm}(r)\,Y_{jm}(\Omega), \qquad \delta\varrho(r,\Omega) = \sum_{jm}\delta\varrho_{jm}(r)\,Y_{jm}(\Omega)$$

Then for $r = a$:

$$\boxed{\delta V_{jm}(a) = \int_{r'=b}^{a} G_j^{sta.}(a,r')\delta\varrho_{jm}(r')dr'}$$

where Green's function of a static geoid is

$$\boxed{G_j^{sta.}(a,r') = \frac{4\pi Ga}{2j+1}\left(\frac{r'}{a}\right)^{j+2}}$$

Green's functions of static geoid ($j = 2, 4, 10$)

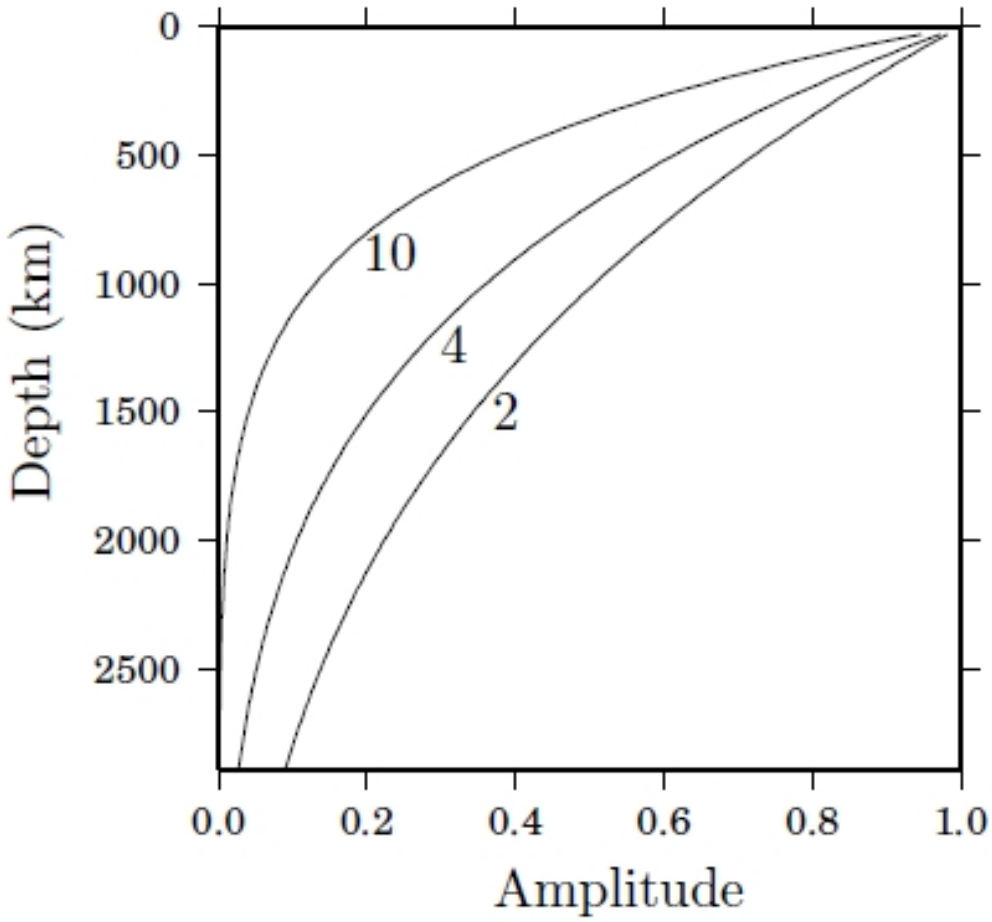

The smaller spatial scales in gravitational potential, the higher sensitivity to shallower small-scale density variations, or in other words, the lower sensitivity to deeper small-scale density variations.

Contents

The Earth's interior is closed to hydrostatic equilibrium

Flattening of the Earth:

- hydrostatic: $f = 1/299.0$
- 'observed': $f = 1/298.257$

$\Rightarrow$ The Earth's 'gravity' interior is slighlty perturbed from the hydrostatic equilibrium:

$$\varrho = \underbrace{\varrho_0}_{\text{hydrostatic}} + \underbrace{\delta\varrho}_{\text{non-hydrostatic}}$$

Additionally:

- Seismic tomographic model of the compressional (P) and transverse (S) seismic elastic waves
- Conversion of seismic anomalies to density anomalies:

$$\frac{\delta\varrho}{\varrho} = p_f \frac{\delta v}{v}$$

p_f ... proportionality factor

The geoid response to a static mantle

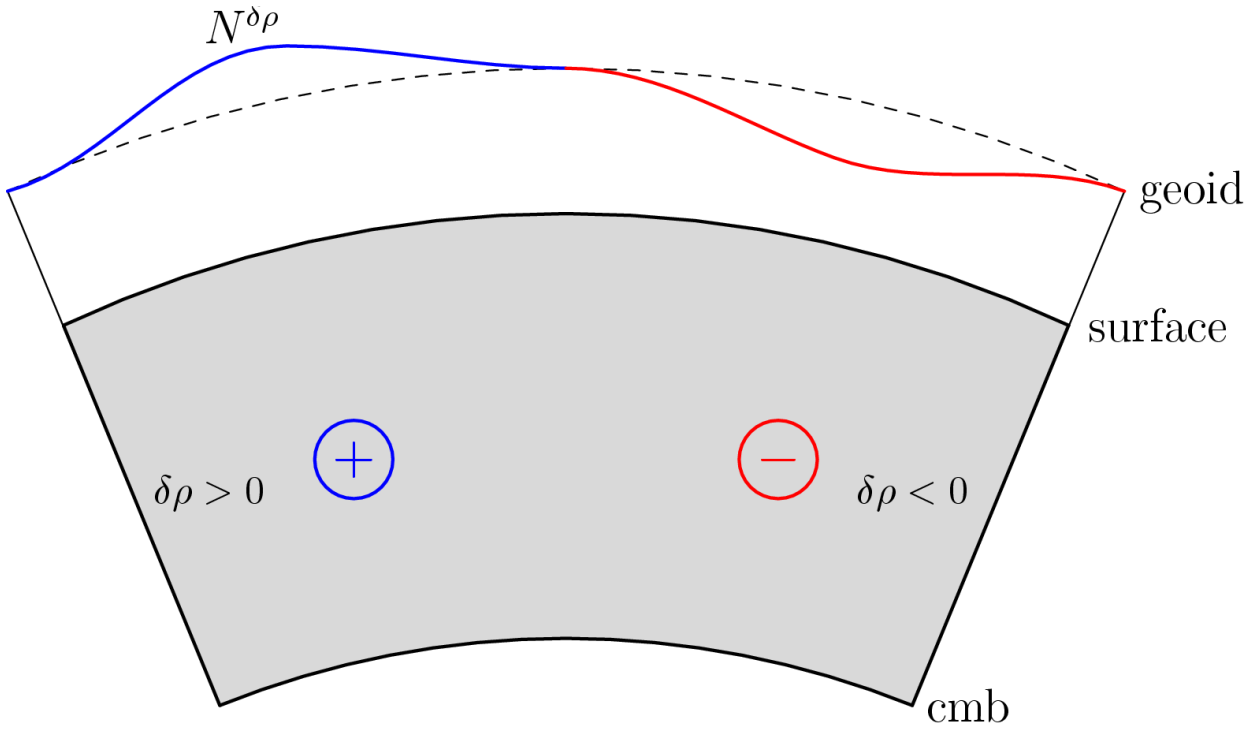

Induced geoid undulations $\sim$ hundreds of meters
$\Rightarrow$ Earth's mantle is **not** static but dynamic

Dynamic mantle

The Earth's mantle is slighlty perturbed from the hydrostatic equilibrium:

$$\begin{aligned} \varrho &= \varrho_0 + \delta\varrho \\ \boldsymbol{g} &= \boldsymbol{g}_0 + \delta\boldsymbol{g} \end{aligned}$$

where

$$\delta\varrho \ll \varrho_0 \quad \text{and} \quad \delta\boldsymbol{g} \ll \boldsymbol{g}_0$$

The gravitational force acting on a material partical:

$$\varrho\boldsymbol{g} \approx \underbrace{\varrho_0\,\boldsymbol{g}_0}_{\text{hydrostatic force}} + \underbrace{\delta\varrho\,\boldsymbol{g}_0}_{\text{buoyancy force}} + \underbrace{\varrho_0\,\delta\boldsymbol{g}}_{\text{self-gravitating force}}$$

Driving forces from equilibrium = buoyancy + self-gravitation

Fluid dynamic model of the geoid

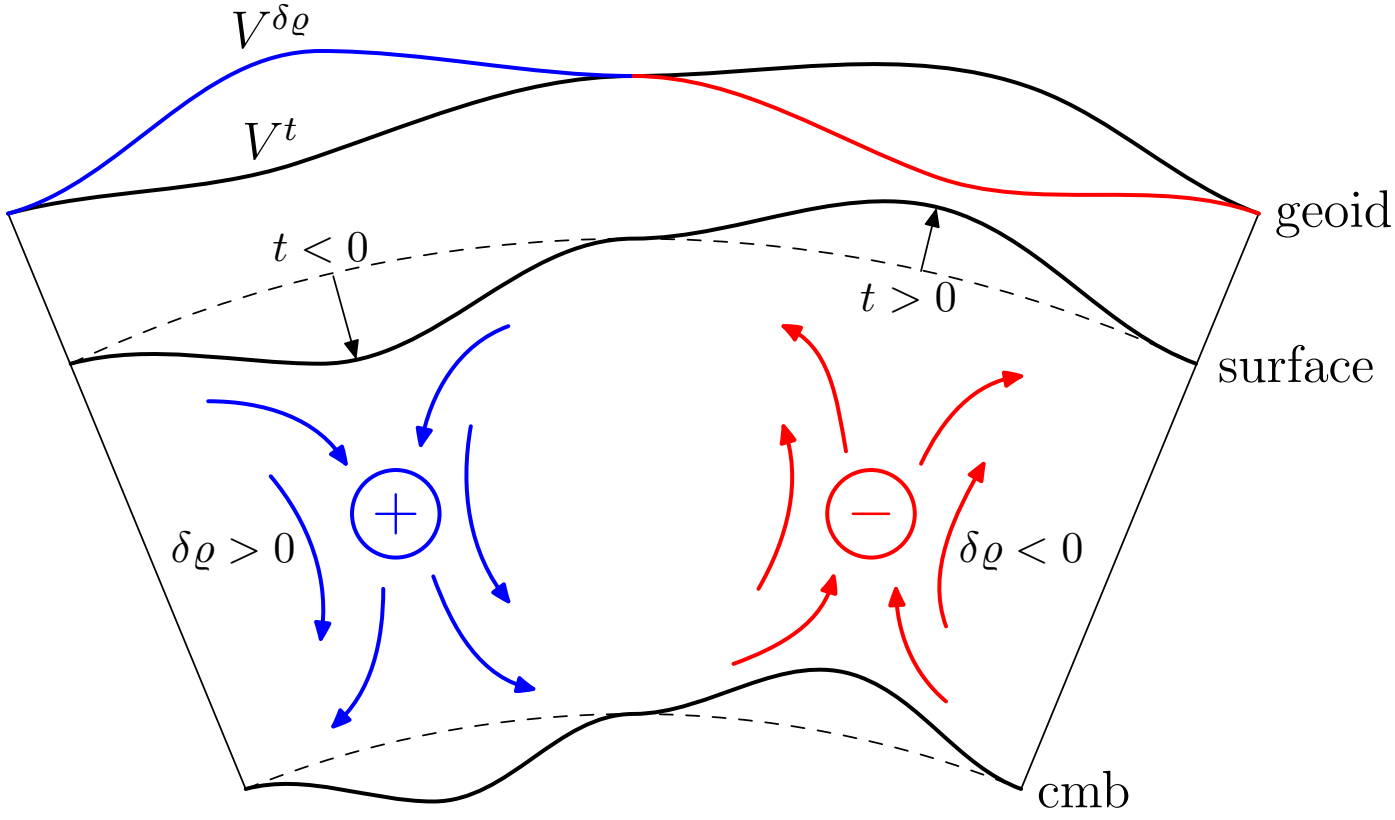

$V^{\delta\varrho}$: potential induced by mantle density anomalies $\delta\varrho$
V^t : potential induced by deformations of boundary topographies t

Courtesy of N.Tosi

Stokes problem for present-day mantle convection

Mass conservation for an incompressible mantle:

$$\mathrm{div}\boldsymbol{v} = 0$$

Momentum conservation with Pr$\rightarrow \infty$:

$$\mathrm{div}\boldsymbol{\tau} + \boldsymbol{f} = 0$$

Constitutive relation for a Newtonian viscous medium:

$$\begin{aligned} \boldsymbol{\tau} &= -p\boldsymbol{I} + 2\eta\boldsymbol{\varepsilon} \\ \boldsymbol{\varepsilon} &= (\nabla\boldsymbol{v} + \nabla^T\boldsymbol{v})/2 \end{aligned}$$

Boundary conditions at $\partial B = \partial B^{top} \cup \partial B^{cmb}$

$$\begin{aligned} \boldsymbol{v}\cdot\boldsymbol{n} &= 0 \\ \boldsymbol{\tau}\cdot\boldsymbol{n} - (\boldsymbol{n}\cdot\boldsymbol{\tau}\cdot\boldsymbol{n})\boldsymbol{n} &= 0 \end{aligned}$$

Weak formulation

Consider a suitable functional space and create the functional

$$F(\boldsymbol{v}, p, \ell_1, \ell_2) = \int_B \eta(\varepsilon : \varepsilon)\, dV + \int_B \boldsymbol{f} \cdot \boldsymbol{v}\, dV + \int_B p \operatorname{div} \boldsymbol{v}\, dV + \int_{\partial B^{top}} \ell_1 (\boldsymbol{n} \cdot \boldsymbol{v})\, dS + \int_{\partial B^{cmb}} \ell_2 (\boldsymbol{n} \cdot \boldsymbol{v})\, dS$$

Compute the variation of F and use of Green's identity

$$\delta F = -\int_B (\operatorname{div} \boldsymbol{\tau} + \boldsymbol{f}) \cdot \delta \boldsymbol{v}\, dV + \int_{\partial B} [\boldsymbol{\tau} \cdot \boldsymbol{n} - (\boldsymbol{n} \cdot \boldsymbol{\tau} \cdot \boldsymbol{n})\boldsymbol{n}] \cdot \delta \boldsymbol{v}\, dS + \int_{\partial B^{top}} (\boldsymbol{n} \cdot \boldsymbol{v})\, \delta \ell_1\, dS + \int_{\partial B^{cmb}} (\boldsymbol{n} \cdot \boldsymbol{v})\, \delta \ell_2\, dS$$

At a stationary point of F, $\delta F = 0$, the differential and the variational problem are equivalent.

Spherical-harmonic, finite-element parameterization

Expansion in *scalar* and *vector* spherical harmonics with respect to **angular coordinates**:

$$p = \sum_{j=0}^{N} \sum_{m=-j}^{j} p_{jm}(r)\, Y_{jm}(\Omega)$$

$$\boldsymbol{v} = \sum_{j=0}^{N} \sum_{m=-j}^{j} [U_{jm}(r)\boldsymbol{S}_{jm}^{(-1)}(\Omega) + V_{jm}(r)\boldsymbol{S}_{jm}^{(1)}(\Omega) + W_{jm}(r)\boldsymbol{S}_{jm}^{(0)}(\Omega)]$$

Expansion into piecewise linear-finite elements with respect to **radial coordinate**:

$$U_{jm}(r) = \sum_{k=1}^{K+1} U_{jm}^{k} \psi_k(r)$$

where:

$$\psi_k(r) = \frac{r_{k+1} - r}{r_{k+1} - r_k} \quad \text{and} \quad \psi_{k+1}(r) = \frac{r - r_{k+1}}{r_{k+1} - r_k}$$

Green's function of geoid for a dynamic mantle

Assumption: 1-D viscosity model $\eta = \eta(r)$.
The gravitational effect of dynamic mantle + dynamic topographies:

$$\delta V(r,\Omega) = G\int_{r'=b}^{a}\int_{\Omega_0}\frac{\delta\varrho(r',\Omega')}{L(r,\psi,r')}r'^2 dr'\,d\Omega' + G\sum_{i=1}^{n}\int_{\Omega_0}\frac{\sigma_i(\Omega')}{L(r,\psi,r_i)}d\Omega'$$

where

$$\sigma_i(\Omega) = \Delta\varrho_i\, t_i(\Omega) \qquad i = 1,...,n$$

and $t_i(\Omega)$ is the i-th dynamic topography. Easy manipulations results in

$$\delta V_{jm}(a) = \int_{r'=b}^{a} G_j^{sta.}(a,r')\delta\varrho_{jm}(r')dr' + \sum_{i=1}^{n}\frac{4\pi Ga}{2j+1}\left(\frac{r_i}{a}\right)^{j+2}\Delta\varrho_i(t_i)_{jm}$$

where t_{jm} are the coefficients of topography $t(\Omega)$. Formally,

$$\boxed{\delta V_{jm}(a) = \int_{r'=b}^{a} G_j^{dyn.}(a,r')\delta\varrho_{jm}(r')dr'}$$

Green's function of a dynamic geoid $G_j^{dyn.}(a,r')$ can only be modelled numerically.

Input data for forward dynamic-mantle modelling

- *S*-wave seismic tomographic model of Becker & Boschi (2002).
- Conversion of seismic to density anomalies:

$$\frac{\delta\varrho}{\varrho} = p_f \frac{\delta v}{v}$$

  proportionality factor $p_f = 0.2$
- 3-layer viscosity model:

$$\begin{array}{lll} & \eta_{LT} = 12.5 \times 10^{21}\,\mathrm{Pa\,s} & r \in (6271 - 6371) \\ VM1: & \eta_{UM} = 1 \times 10^{20}\,\mathrm{Pa\,s} & r \in (5701 - 6271) \\ VM2: & \eta_{UM} = 5 \times 10^{20}\,\mathrm{Pa\,s} & r \in (5701 - 6271) \\ & \eta_{LM} = 40 \times \eta_{UM} & r \in (3471 - 5701) \end{array}$$

Green's functions of dynamic geoid ($j = 2, 8, 1630$)

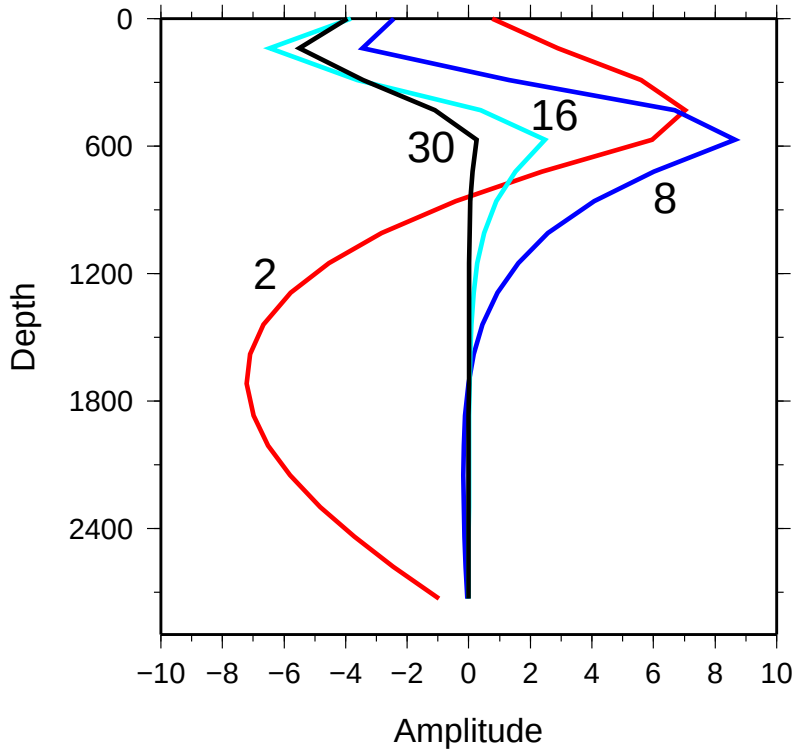

Green's functions of surface dynamic topography ($j = 2, 8, 16, 30$)

TBD

Geoid

GOCO02 (j=2−12)

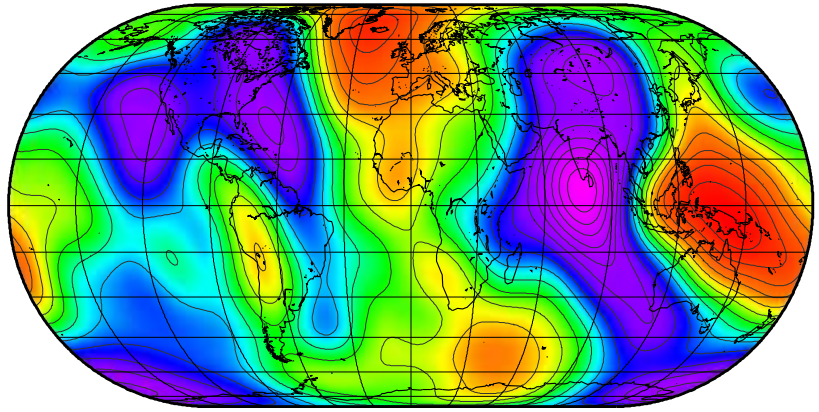

SMEAN model

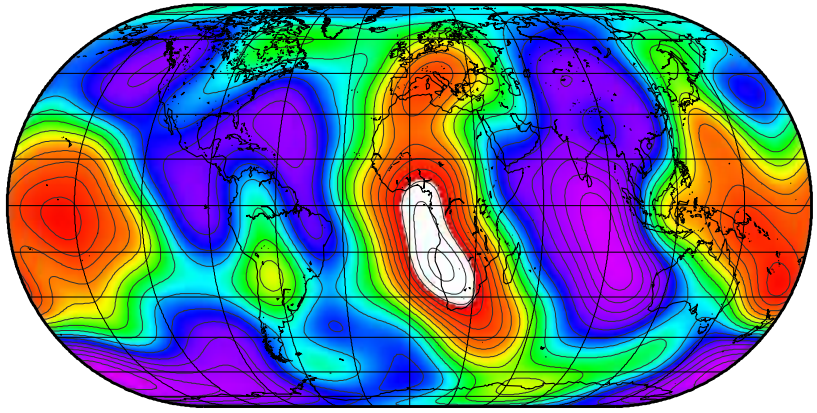

LB model

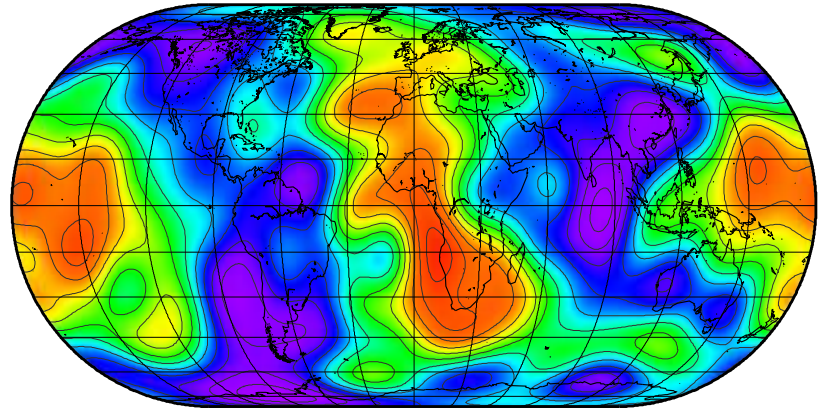

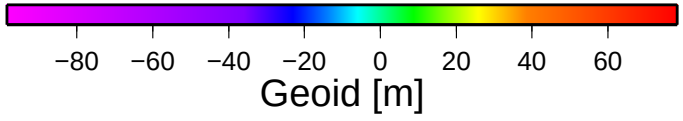

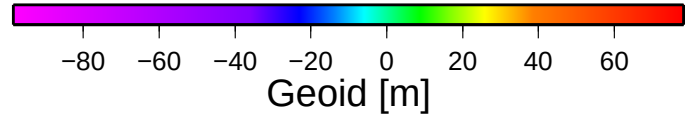

Surface dynamic topography

SMEAN model

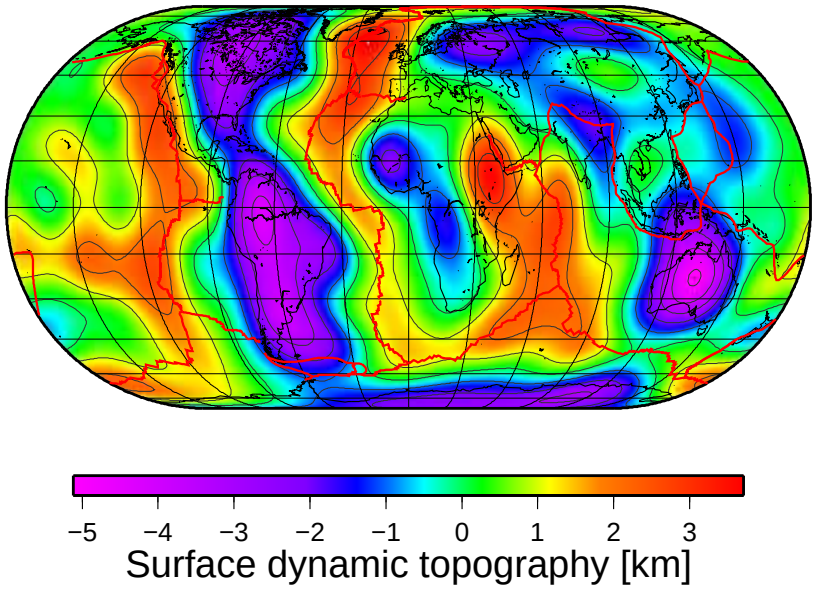

LB model

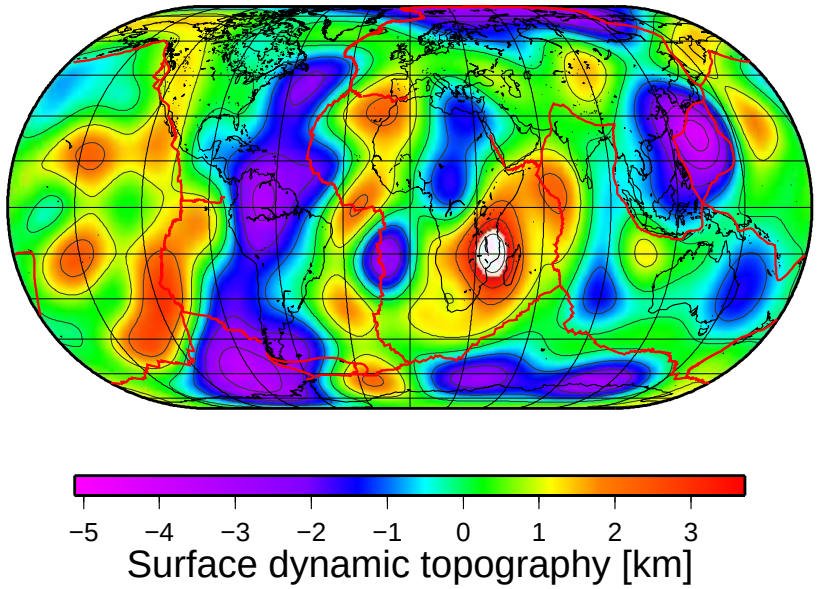

CMB dynamic topography

SMEAN model

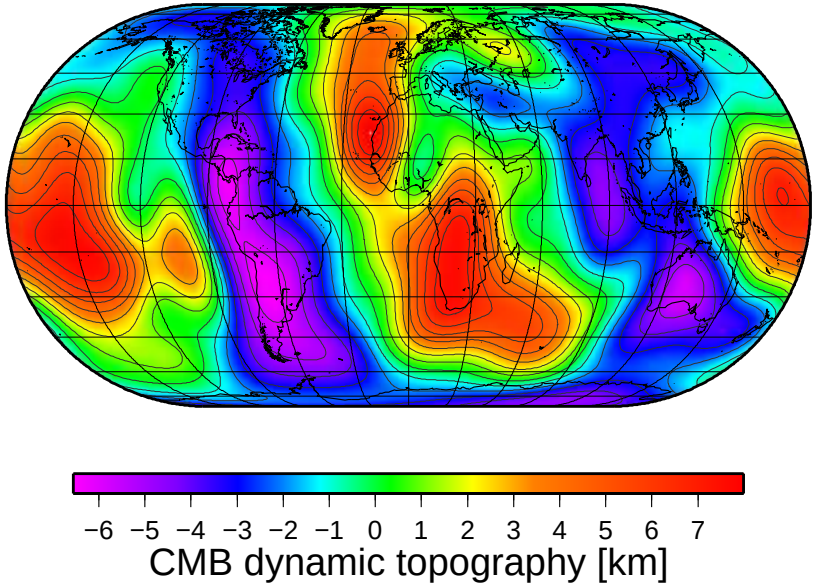

LB model

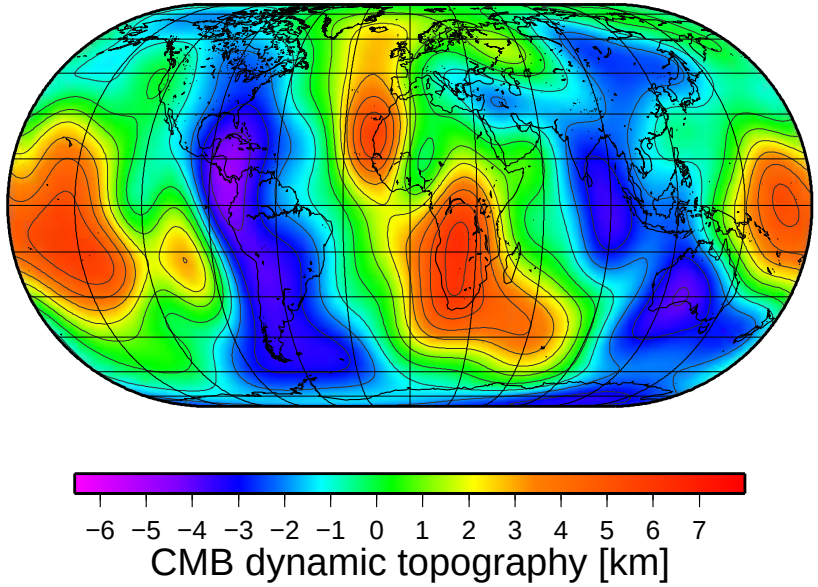

SMEAN dynamic-mantle prediction

SMEAN (j=2−30)

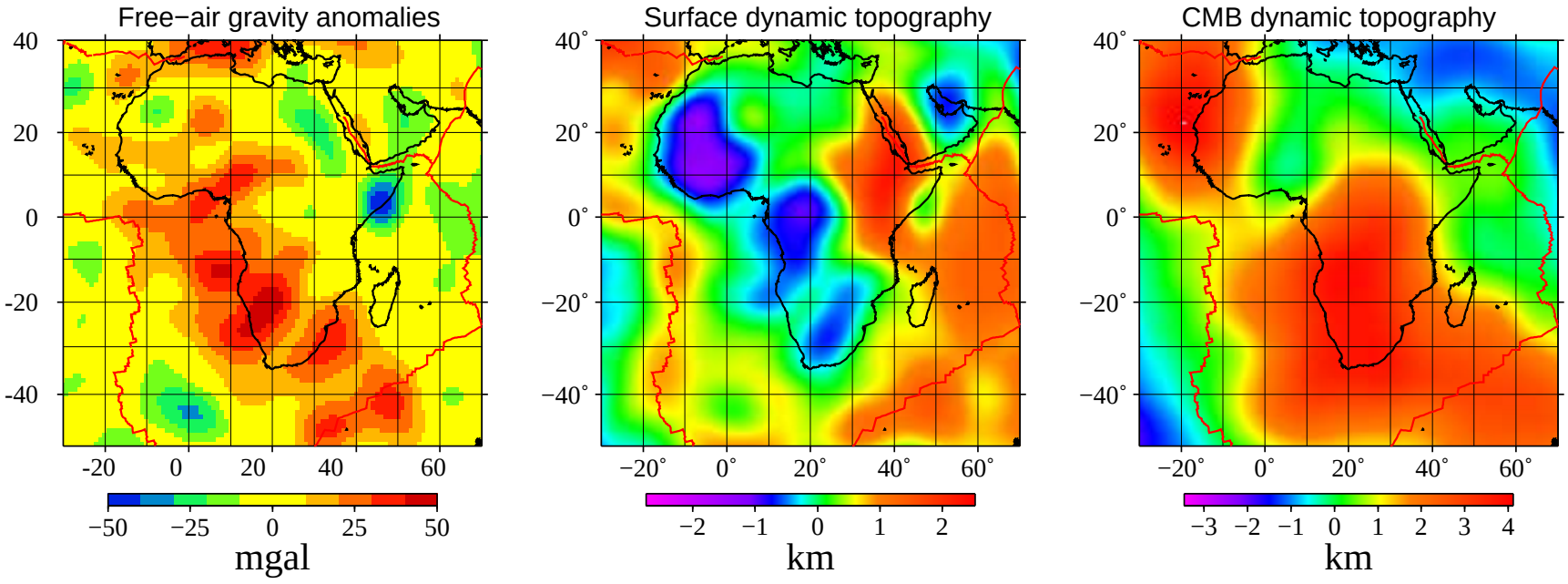

Observed vs. predicted g-fields

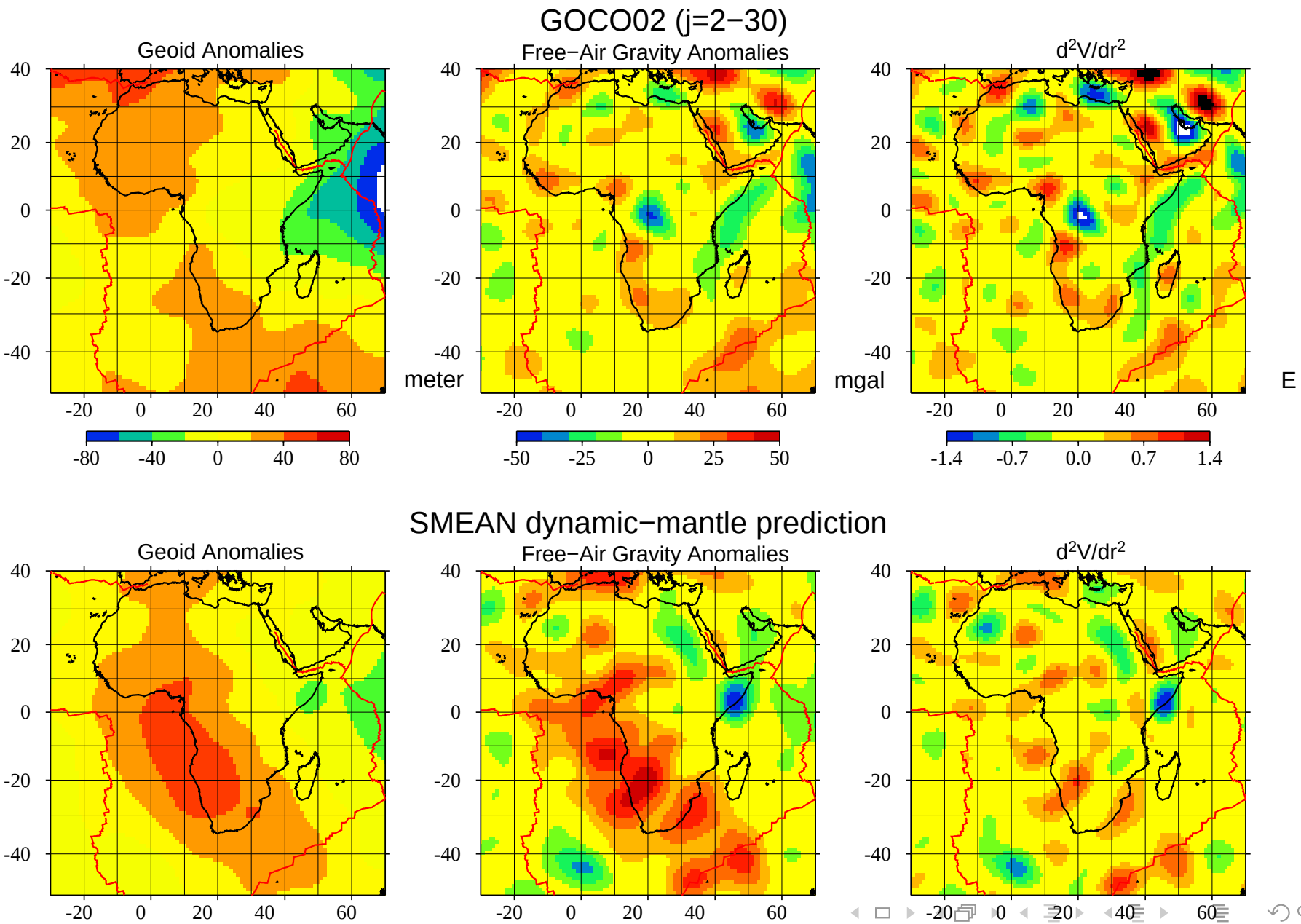

SMEAN dynamic-mantle prediction: VM1 vs. VM2

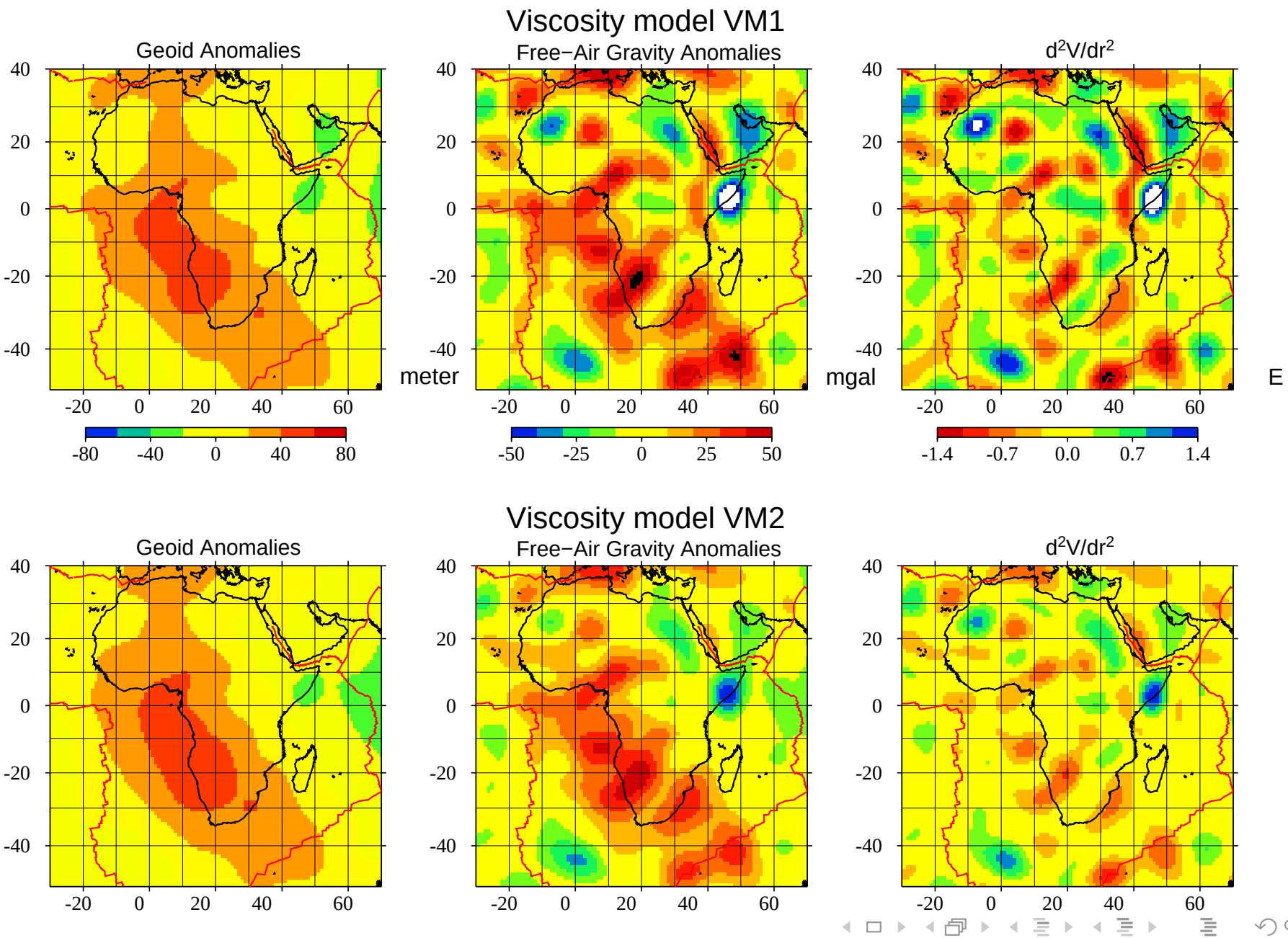

Contents

Tomography of crust & shallow UM (Lebedev & Hilst, 2008)

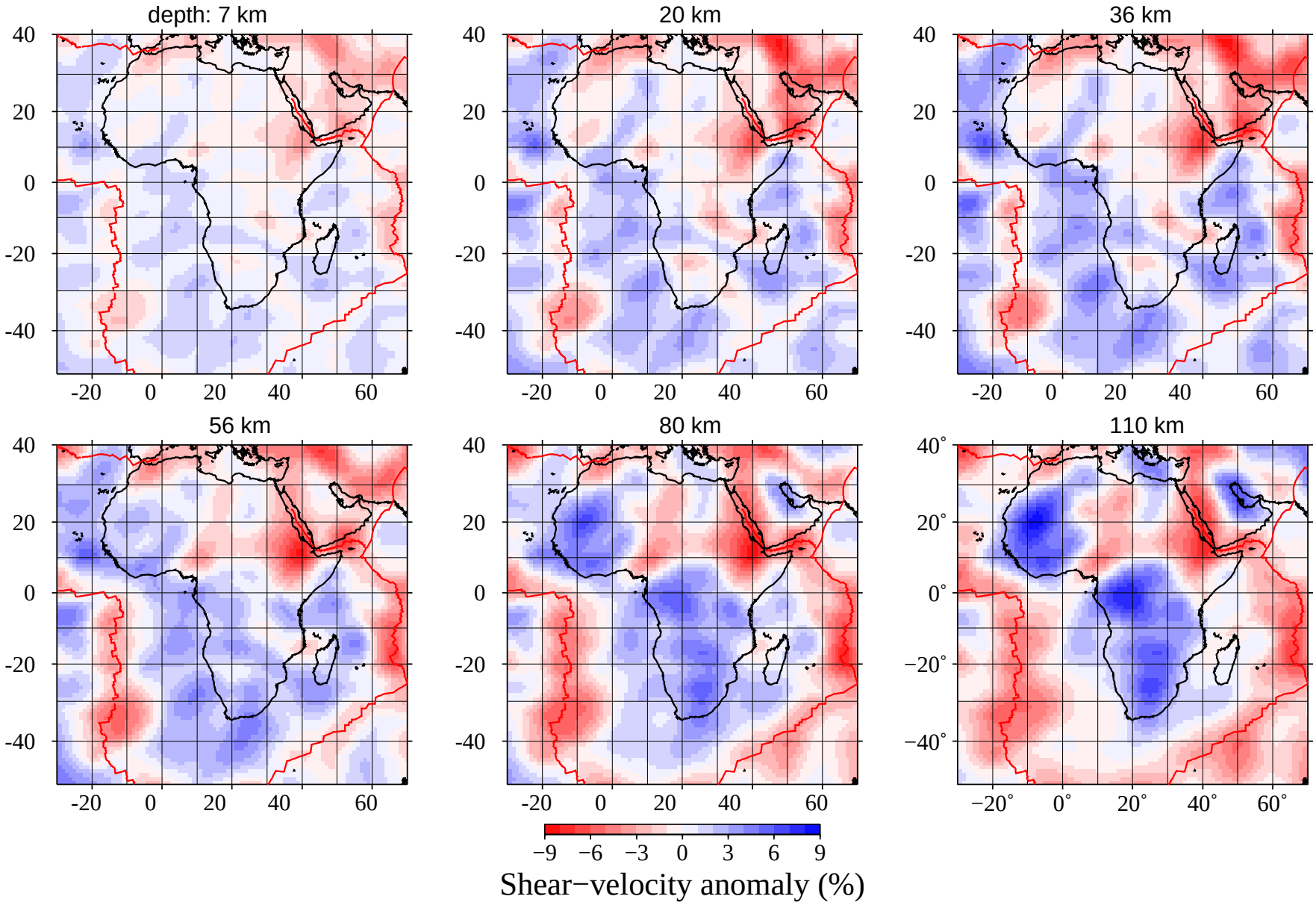

Tomography of deep UM (Lebedev & Hilst, 2008)

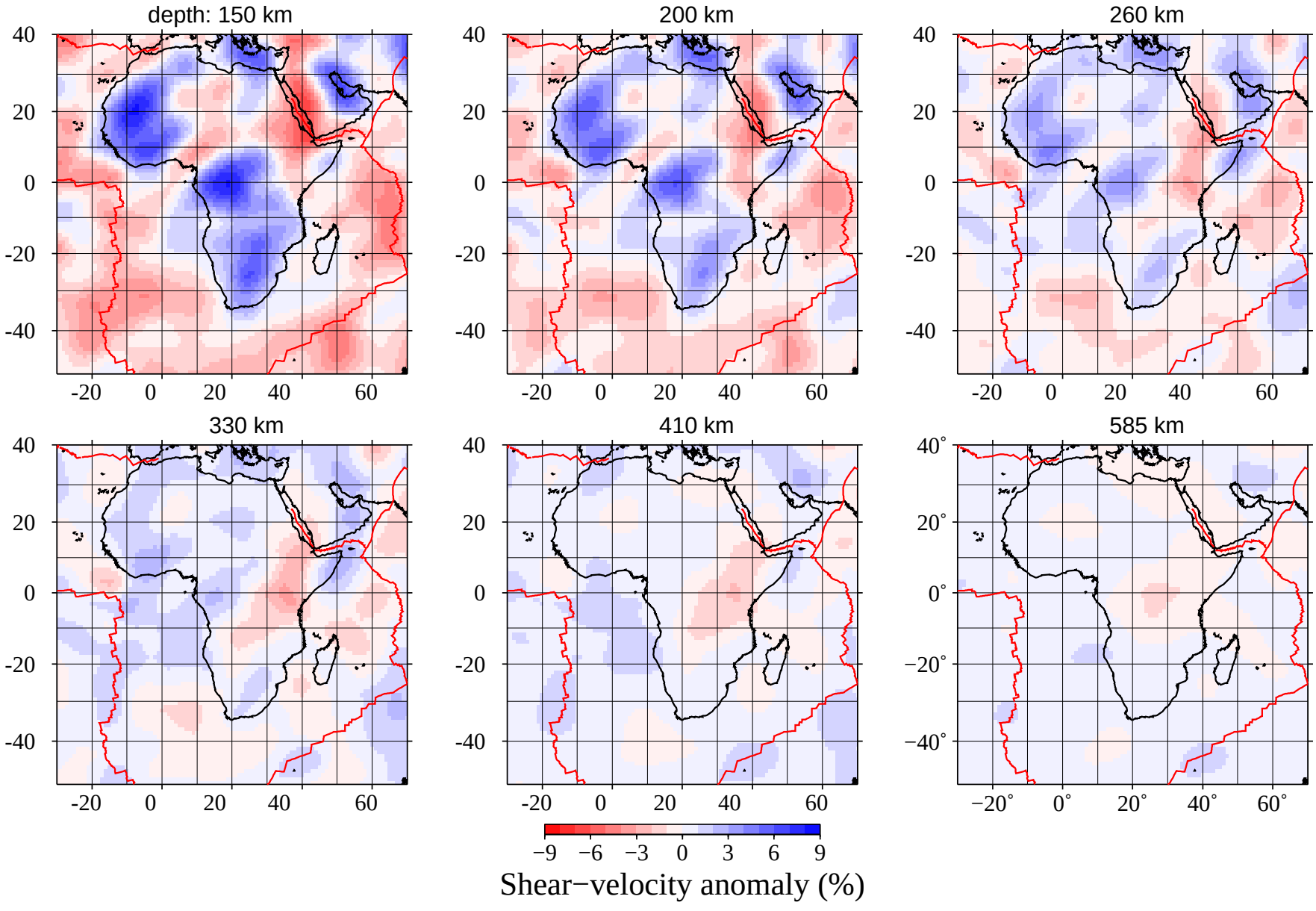

Lithospheric thickness

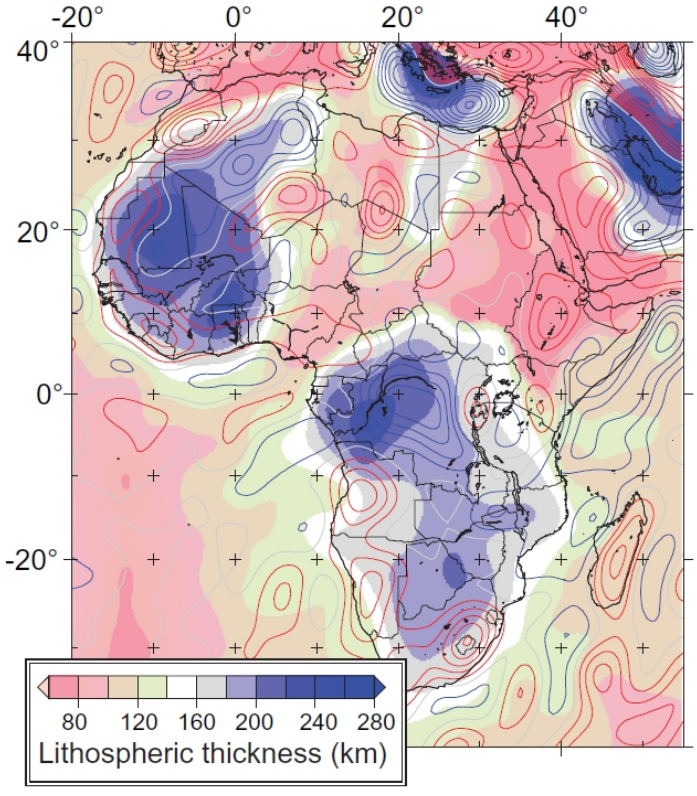

Fishwick & Bastow, 2011

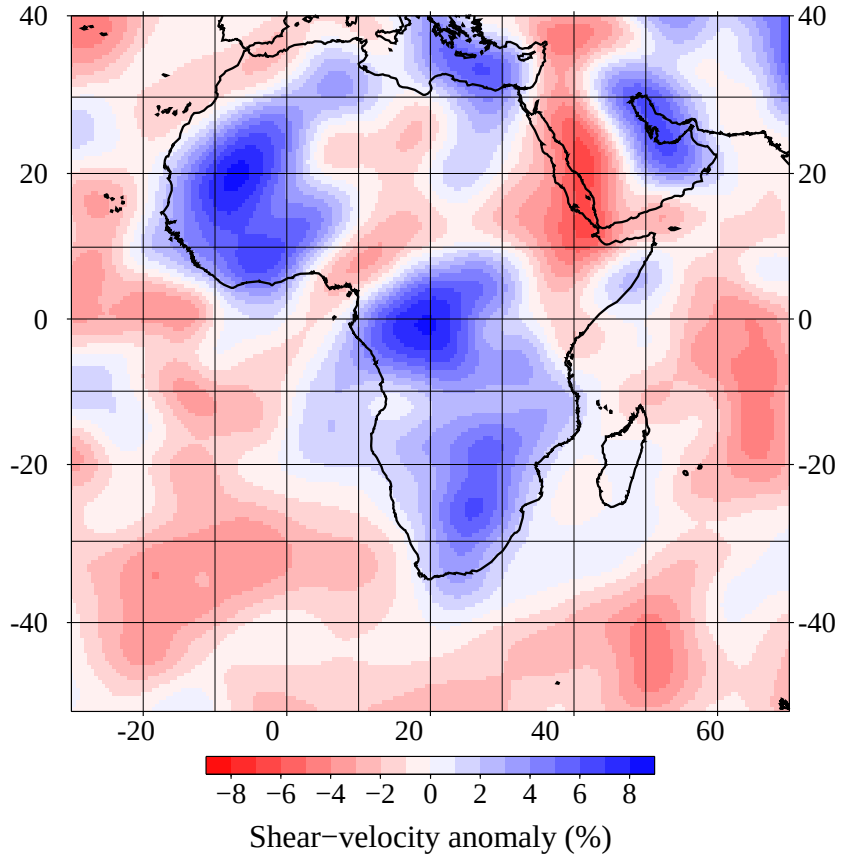

Lebedev & Hilst, 2008

Contents

Free-air gravity anomalies

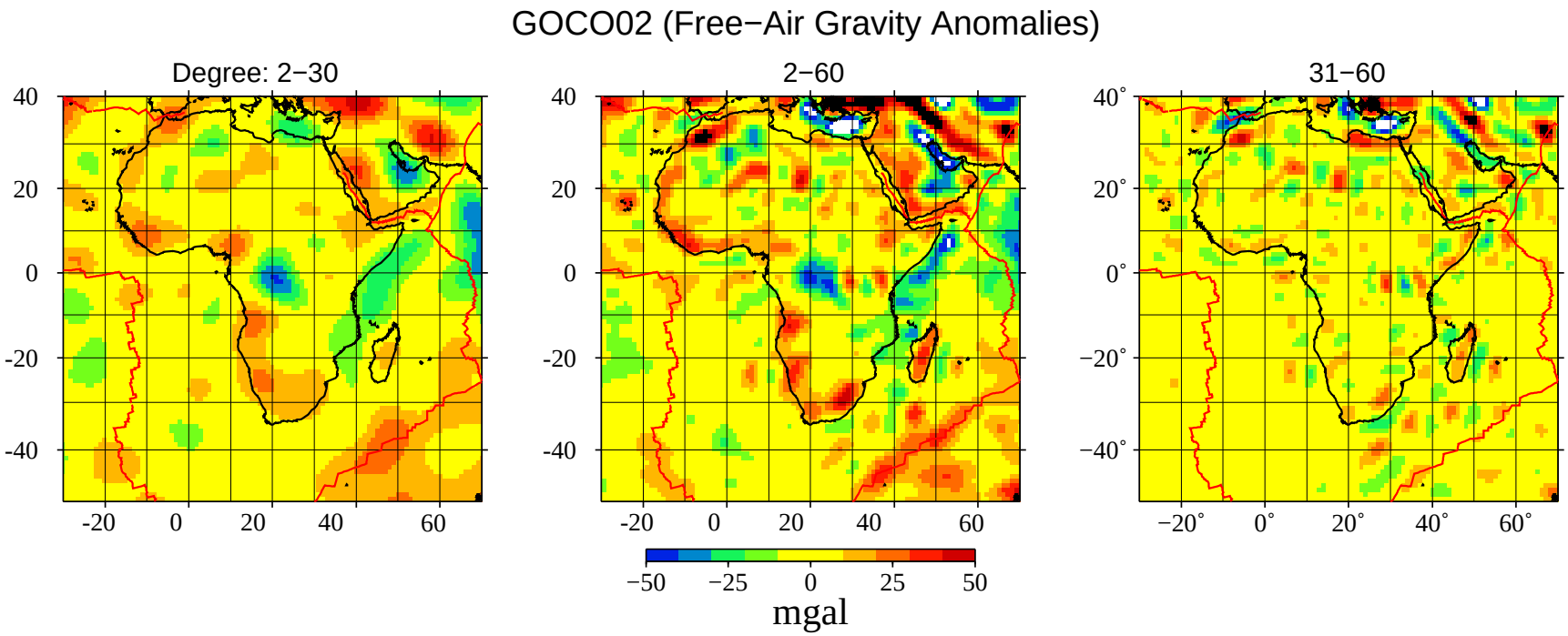

Butterworth filter

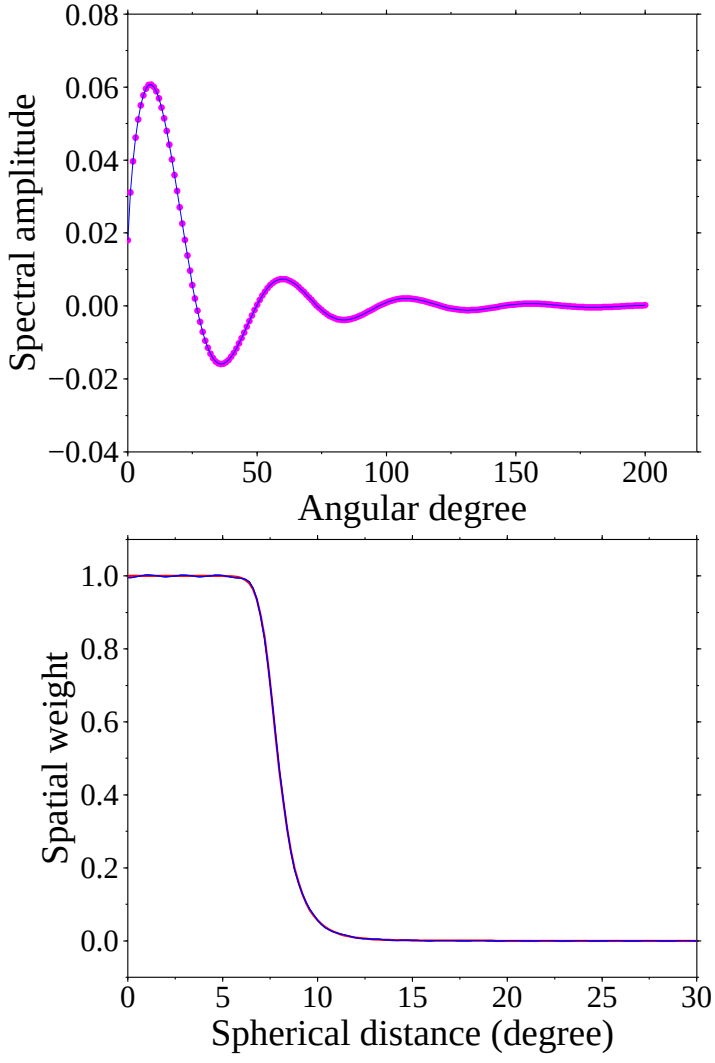

Cut-off frequency = 7.5 deg

Masked GOCO02 free-air gravity anomalies

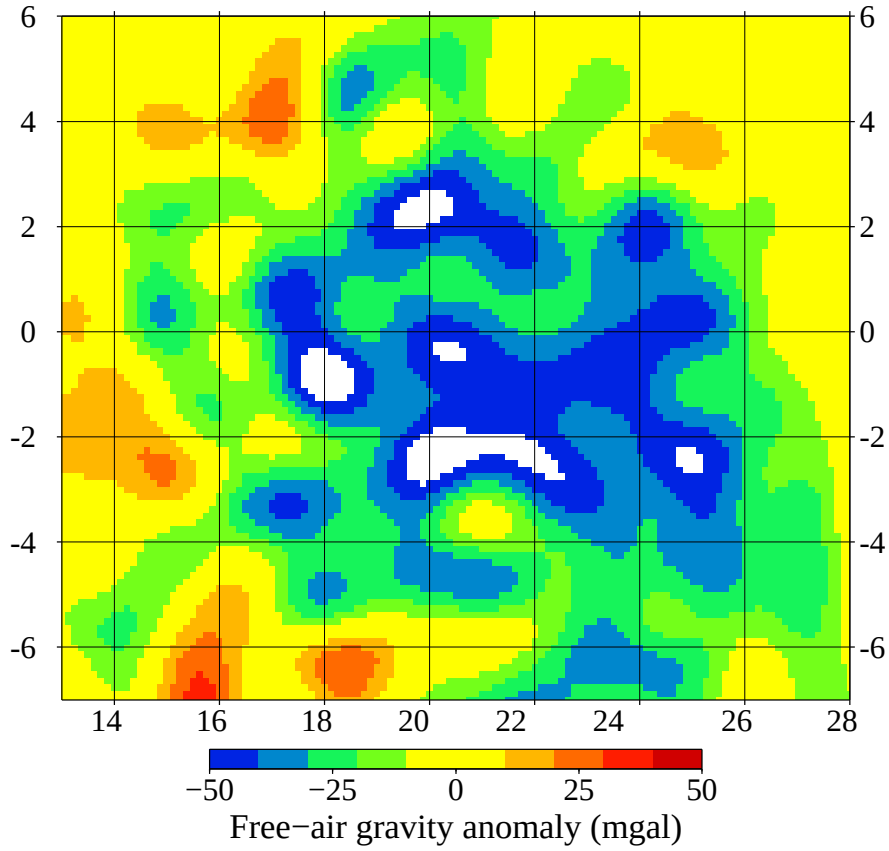

$j_{max} = 180$

Possible contributors to the (static) gravity field

- Surface topography (Is $\varrho = 2670$ kg/m^3 correct for sedimentary basin?)
- Lower-density sediments
- 3-D density variations within the crust (various geological units)
- Compensation at the Moho discontinuity
- 1-D (3-D) density variations in the lithosphere
- Compensation at the lithosphere boundary
- Pull-down or push-up by mantle flow at the lithosphere boundary
- 3-D density variations due to mantle convection
- ...

ETOPO1 topography

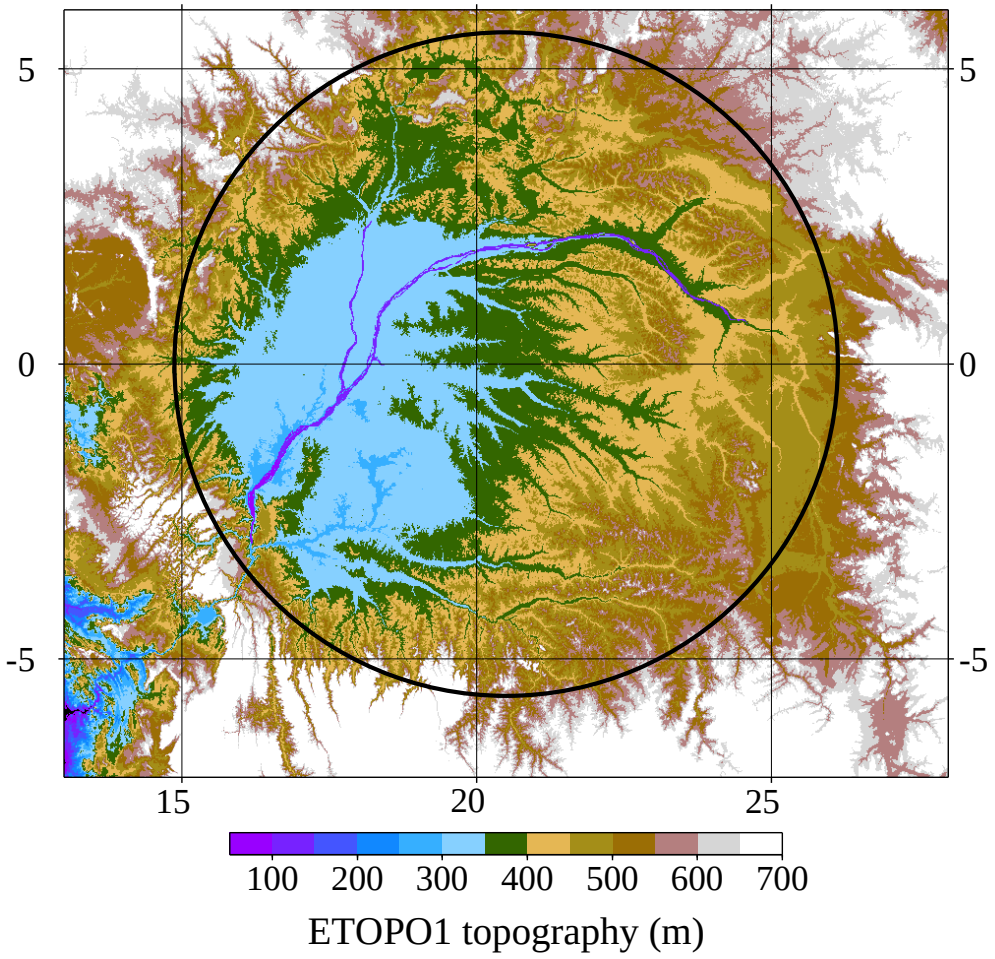

Total sediment thickness of Congo basin

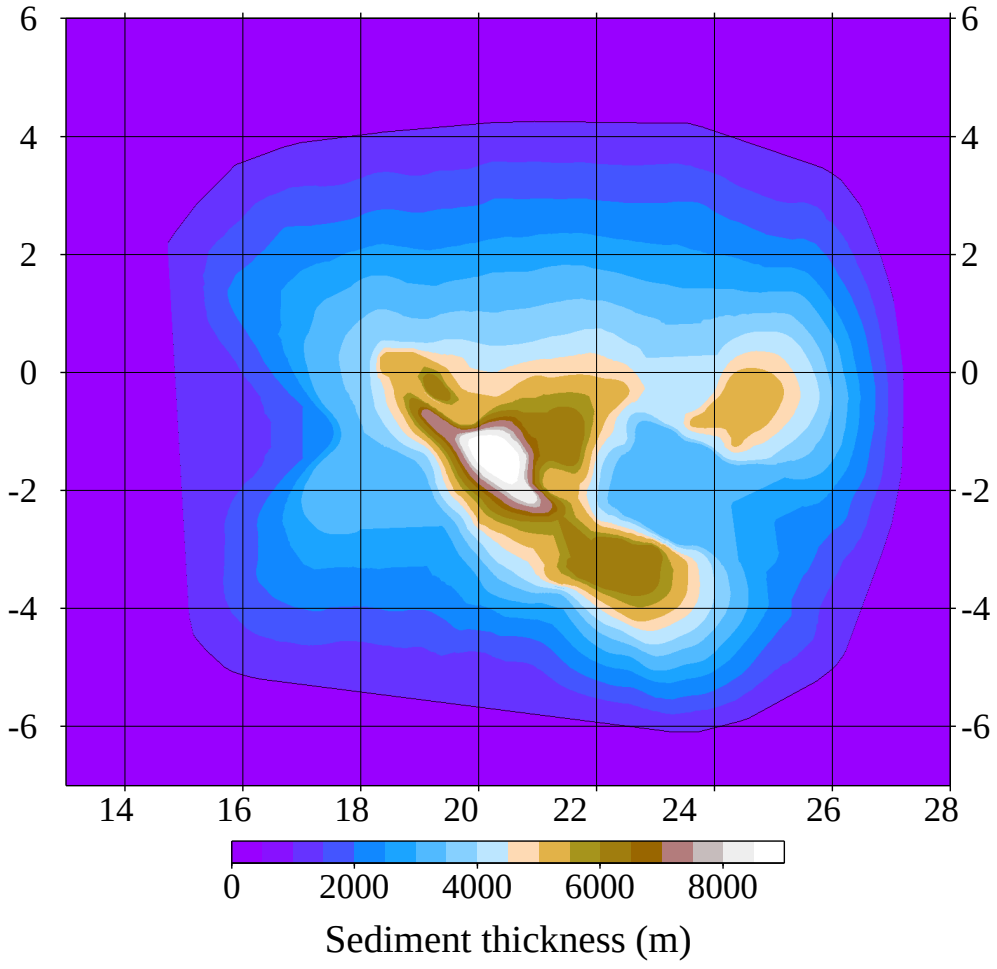

Kadima et *al.*, 2011

Degree amplitude spectra

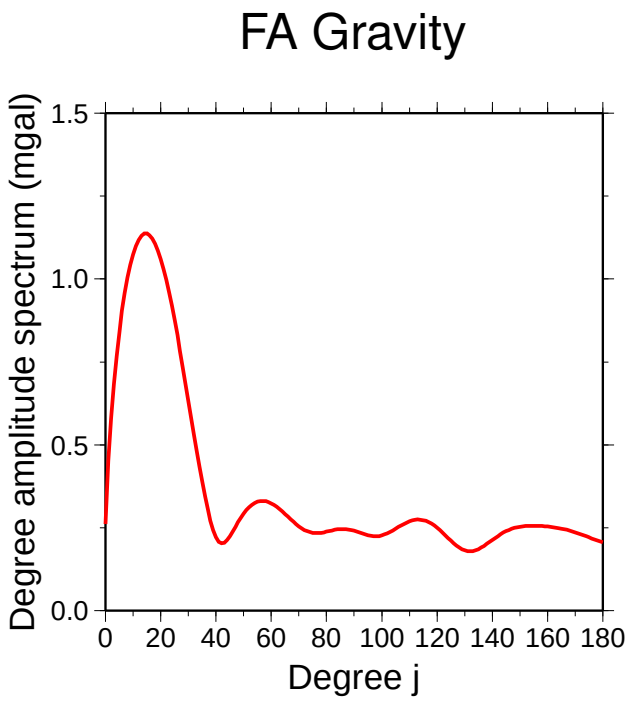

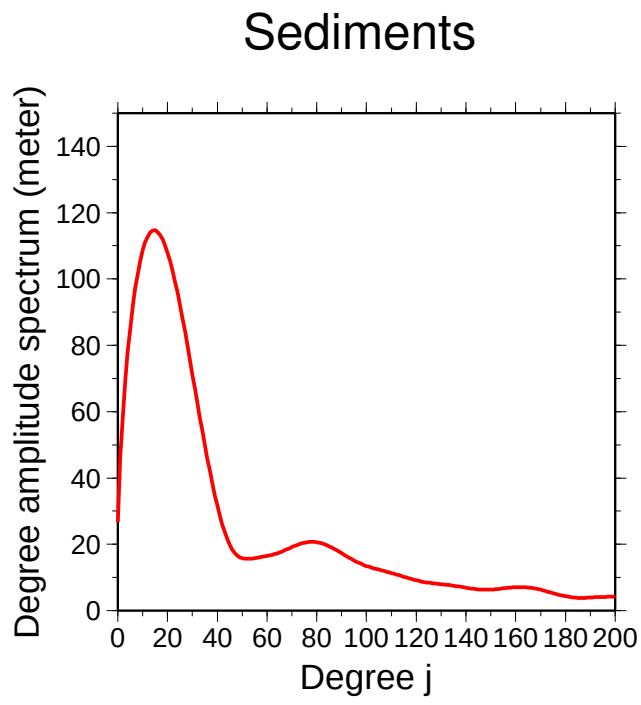

A density contrast

The external gravitation of a body can be approximated by a material surface with either surface mass density

$$\sigma(\Omega) = \begin{cases} \Delta\varrho\, t(\Omega) & \text{Airy's type} \\ \\ h\,\varrho(\Omega) & \text{Pratt's type} \end{cases}$$

The coefficients of the gravity induced by Airy's type mass surface:

$$g_{jm}^{\Delta\varrho} = (j+1)\Delta\varrho T_{jm} \qquad T_{jm} = \frac{3}{a\,\varrho_{mean}} \frac{t_{jm}}{2j+1}$$

Let R_{jm} be the residual gravity coefficients:

$$R_{jm} = g_{jm}^{obs} + g_{jm}^{\Delta\varrho}$$

The density contrast $\Delta\varrho$ will be searched by minimization of R_{jm}:

$$\sum_{jm} R_{jm} R_{jm}^{*} = \min_{\Delta\varrho}$$

It results in (Martinec, 1994):

$$\boxed{\Delta\varrho = -\frac{\sum_{jm}(j+1)\,T_{jm}\,g_{jm}^{obs\,*}}{\sum_{jm}(j+1)^2\,T_{jm}\,T_{jm}^{*}}}$$

Degree correlation and density contrast

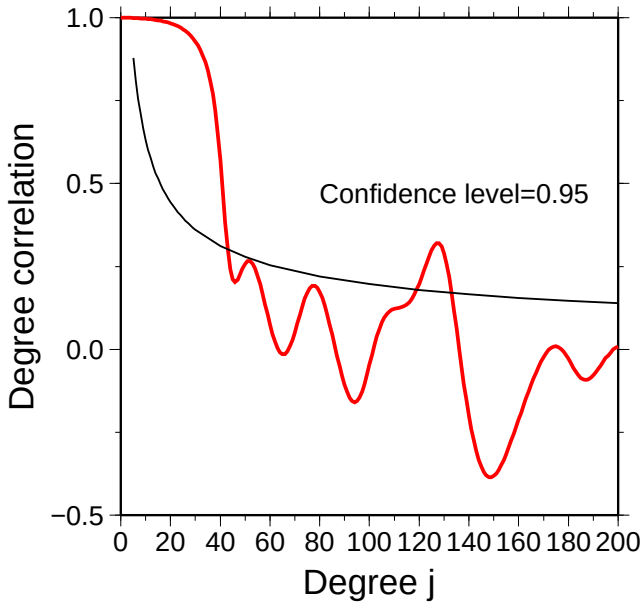

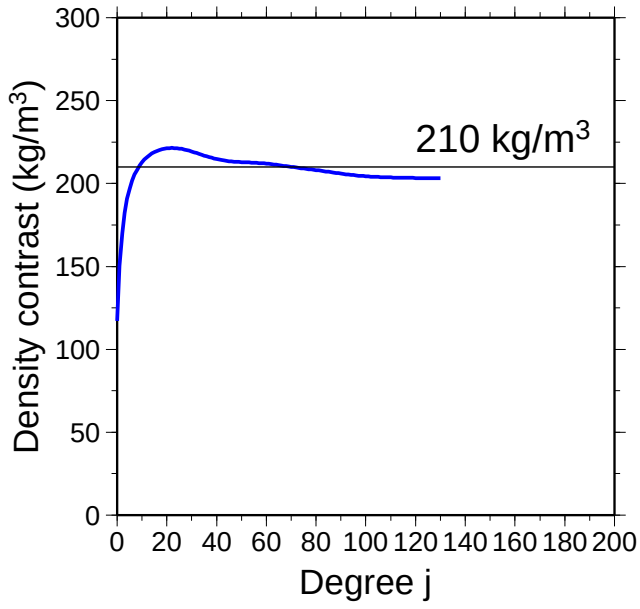

Conclusions:

- Free-air gravity and gravity induced by sediments are correlated (in sense of statistical significance) up to degree $j = 130$
- The density of sediments is in average of 210 kg/m^3 smaller than the density of surrounding crustal material

Gravity signals, $j_{max} = 130$

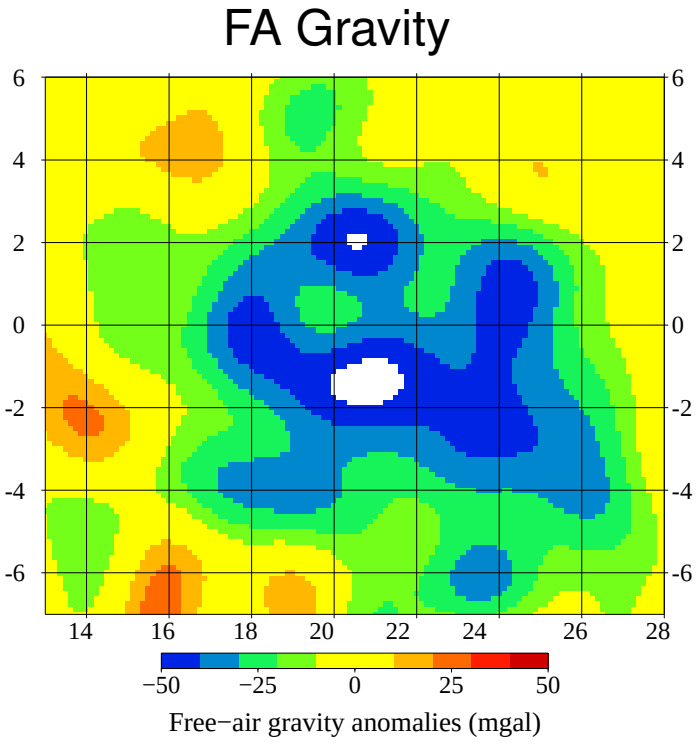

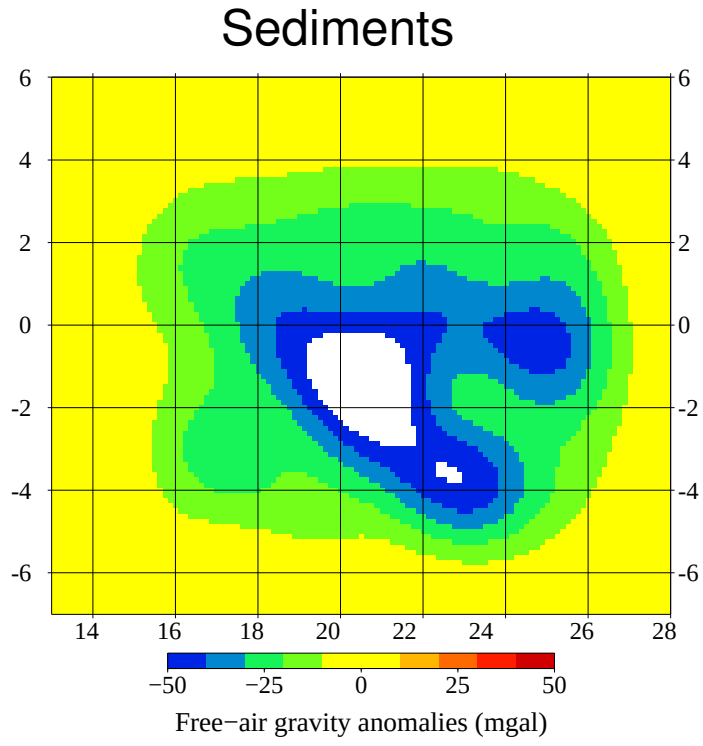

Residual free-air gravity, $j_{max} = 130$

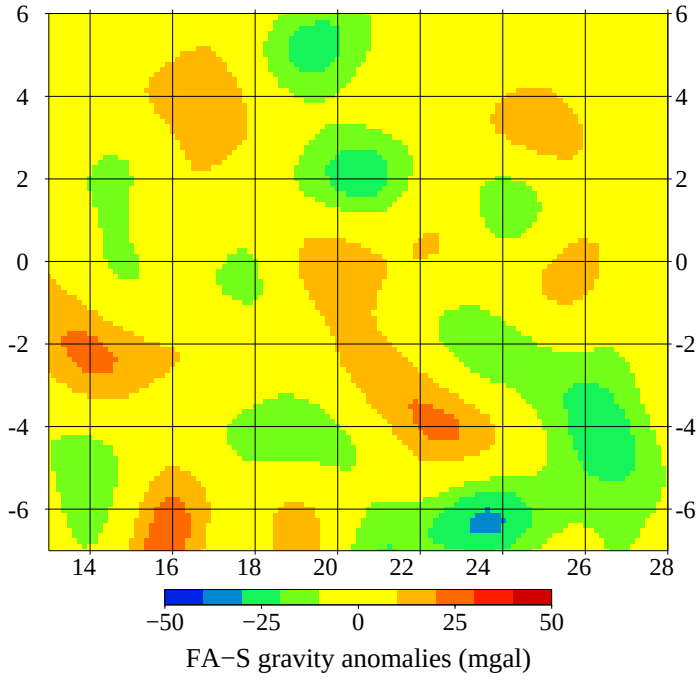

Kadima et *al*. (2011) hypothesis: Uplift of the Moho surface $\Rightarrow$
$\Rightarrow$ crustal thickening $\Rightarrow$ fill in by heavier mantle material

The effect of topography, $j_{max} = 130$

Bouguer gravity corrections

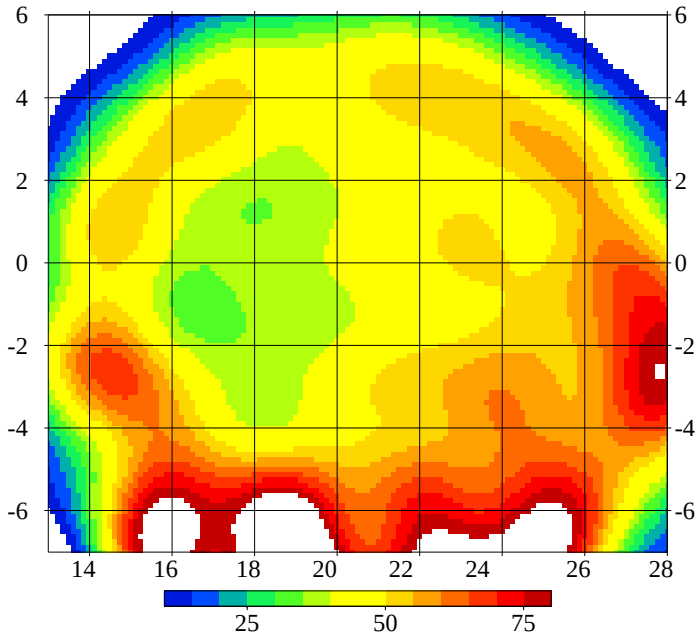

Geological units

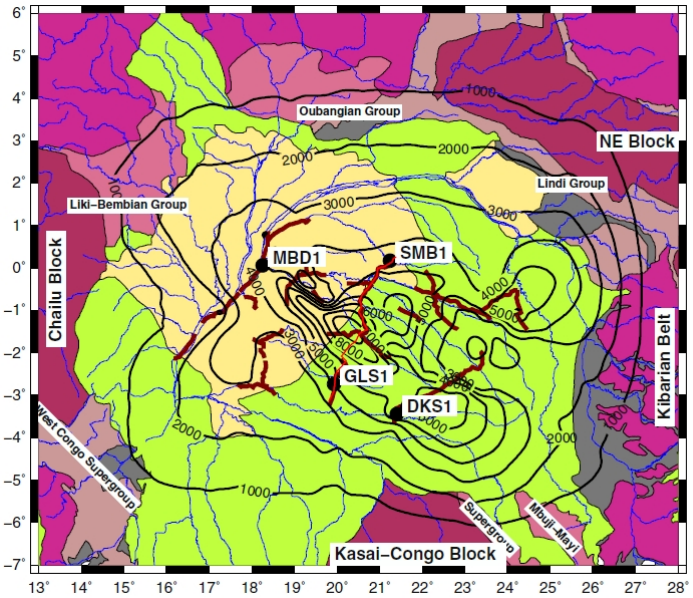

Kadima et *al.*, 2011

The crustal thickness over Africa

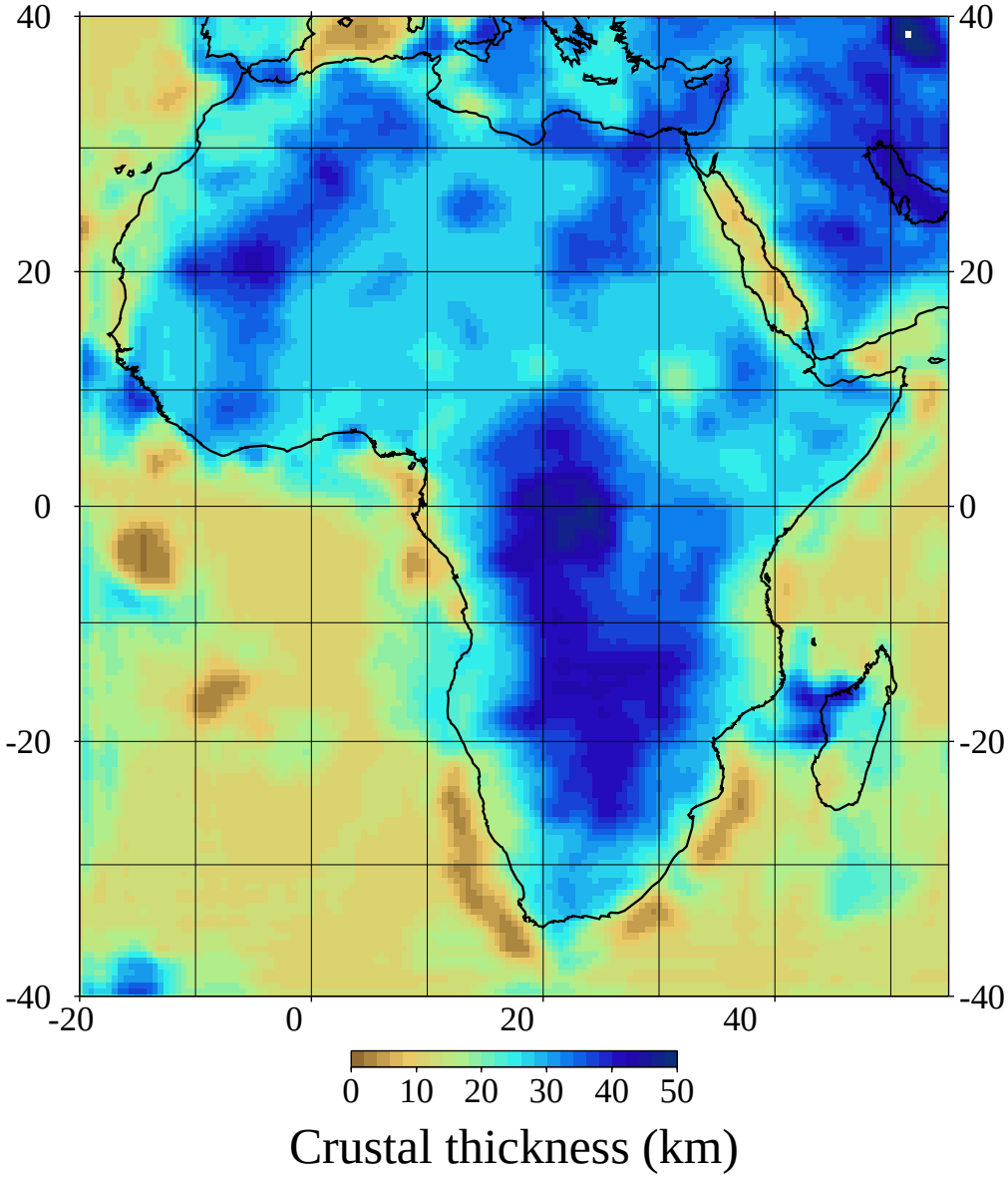

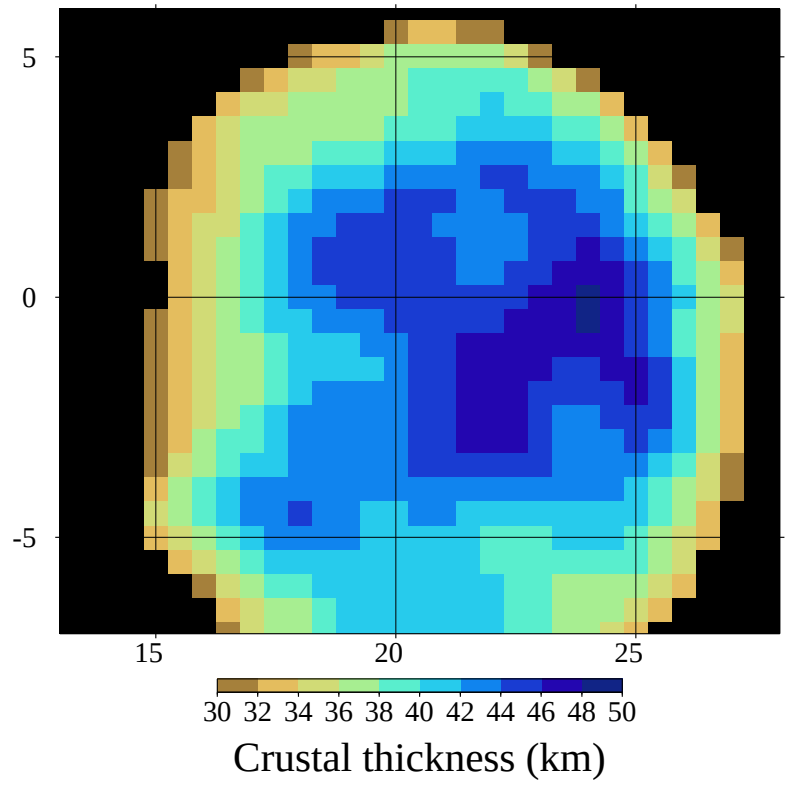

Pasyanos & Nyblade, 2007

The Moho-induced gravity, $j_{max} = 180$

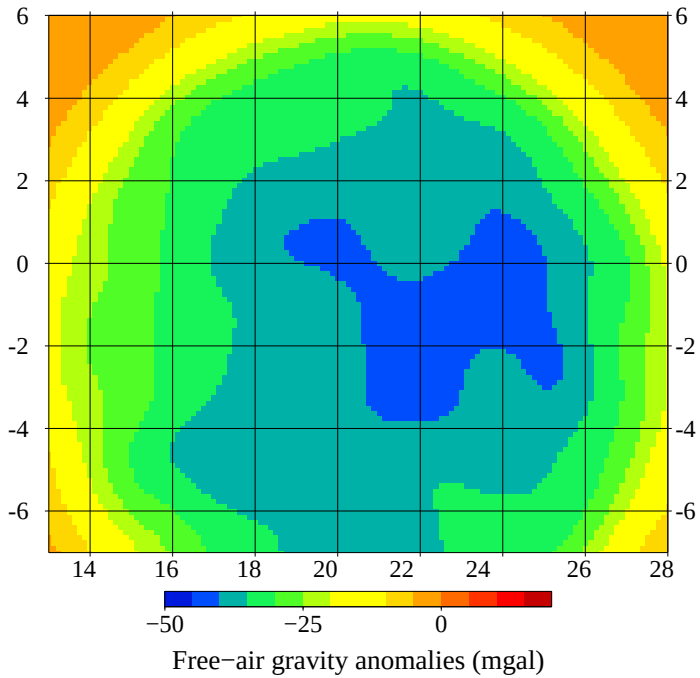

$\Delta\varrho_{Moho} = 20$ kg/m^3

A possible scenario

- The negative free-air gravity could be explained by lower-density sediments (it agrees with Kadima et *al*., 2011), except the narrow, NW-SE oriented, positive gravity anomaly.
- The positive Bouguer gravity correction could be balanced by the negative Moho-induced gravity. However, the narrow, NW-SE oriented, positive gravity anomaly is amplified, not compensated (it contradicts to Kadima et *al*., 2011 hypothesis).
- The Congo high-seismic velocity lithospheric craton may have a large density (due to thermal reason) and induced a higher gravity could be compensated by the negative gravity induced by mantle flow (not shown here, but also within the frame of Buiter at *al*., 2011)

Open question: How to interpret the narrow, NW-SE oriented, positive gravity anomaly?

Contents

Gravitational potential and its gradients

$$
\begin{aligned}
V(\vec{r}) &= \kappa \int_{\mathcal{B}} \varrho(\vec{r'})\, G(\vec{r},\vec{r'})\, dV \\
\operatorname{grad} V(\vec{r}) &= \kappa \int_{\mathcal{B}} \varrho(\vec{r'})\, \vec{G}(\vec{r},\vec{r'})\, dV \\
\operatorname{grad}\operatorname{grad} V(\vec{r}) &= \kappa \int_{\mathcal{B}} \varrho(\vec{r'})\, \boldsymbol{G}(\vec{r},\vec{r'})\, dV
\end{aligned}
$$

Green's functions:

$$
\begin{aligned}
G(\vec{r},\vec{r'}) &:= \frac{1}{L(r,\psi,r')} \\
\vec{G}(\vec{r},\vec{r'}) &:= \operatorname{grad}\frac{1}{L} = -\frac{\vec{r}-\vec{r'}}{L^3} \\
\boldsymbol{G}(\vec{r},\vec{r'}) &:= \operatorname{grad}\operatorname{grad}\frac{1}{L} = -\frac{1}{L^3}\left[\boldsymbol{I} - \frac{3(\vec{r}-\vec{r'})\otimes(\vec{r}-\vec{r'})}{L^2}\right]
\end{aligned}
$$

An example in 2-D Cartesian geometry

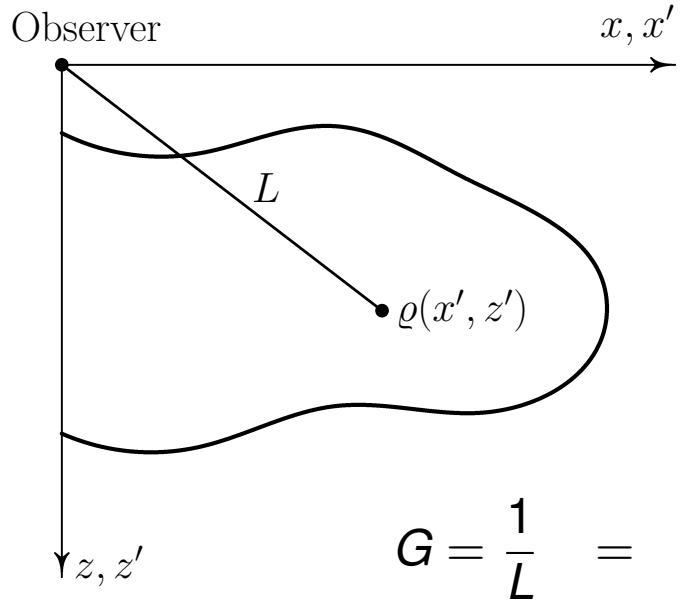

Green's functions at $(x = 0, z = 0)$:

$$G = \frac{1}{L} = \frac{1}{\sqrt{x'^2 + z'^2}}$$

$$G_x = \left(\text{grad}\,\frac{1}{L}\right)_x = \frac{x'}{L^3}$$

$$G_z = \left(\text{grad}\,\frac{1}{L}\right)_z = \frac{z'}{L^3}$$

$$G_{xx} = \left(\text{grad grad}\,\frac{1}{L}\right)_{xx} = -\frac{1}{L^3}\left(1 - \frac{3x'^2}{L^2}\right)$$

$$G_{xz} = \left(\text{grad grad}\,\frac{1}{L}\right)_{xz} = \frac{3x'z'}{L^5}$$

$$G_{zz} = \left(\text{grad grad}\,\frac{1}{L}\right)_{zz} = -\frac{1}{L^3}\left(1 - \frac{3z'^2}{L^2}\right)$$

Scalar, vector and tensor Green's functions for mass density

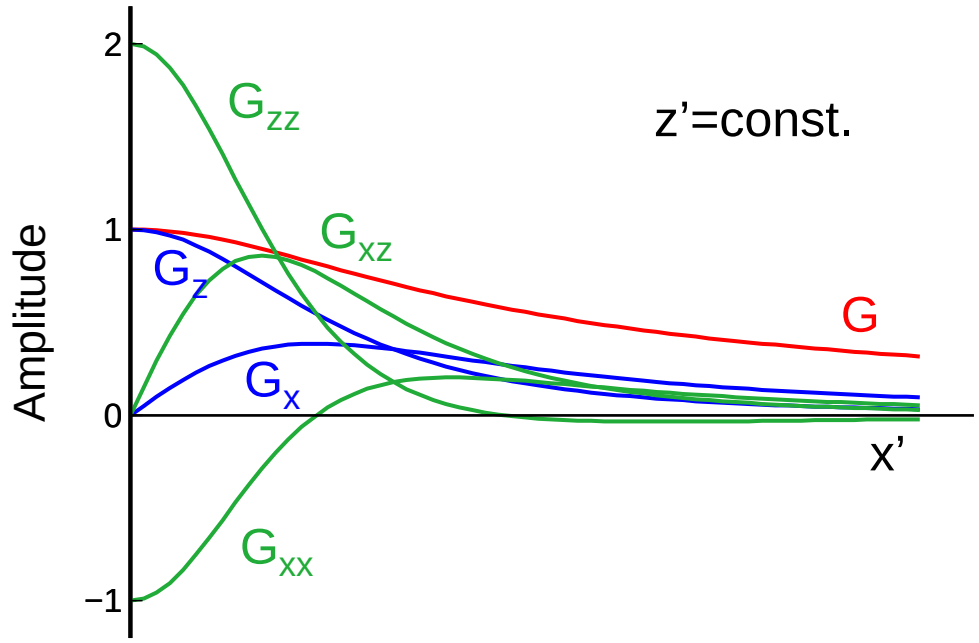

Conclusion: The higher the order of the derivative of the gravitational potential as a boundary datum, the smaller the contribution from far-zone mass-density anomalies.

Mass-density Green's functions for gradiometric data in spherical geometry

After lengthy derivation:

$$\operatorname{grad}\operatorname{grad}\frac{1}{L}=\frac{1}{r^3}\left[K_{rr}(t,x)\boldsymbol{e}_{rr}+K_{r\Omega}(t,x)(\cos\alpha\,\boldsymbol{e}_{r\vartheta}-\sin\alpha\,\boldsymbol{e}_{r\varphi})\right.$$
$$\left.+K_{\Omega\Omega}(t,x)\Big(\cos 2\alpha\;(\boldsymbol{e}_{\vartheta\vartheta}-\boldsymbol{e}_{\varphi\varphi})-2\sin 2\alpha\,\boldsymbol{e}_{\vartheta\varphi}\Big)-\frac{1}{2}K_{rr}(t,x)\,(\boldsymbol{e}_{\vartheta\vartheta}+\boldsymbol{e}_{\varphi\varphi})\right]$$

ψ ... spherical distance, $x=\cos\psi$
α ... azimuth
$t=r'/r$

Three isotropic kernels:

$$\begin{aligned}
K_{rr}(t,x) &= \sum_{j=0}^{\infty}(j+1)(j+2)t^jP_j(x)\\
K_{r\Omega}(t,x) &= -2\sqrt{1-x^2}\sum_{j=0}^{\infty}(j+2)t^j\frac{dP_j(x)}{dx}\\
K_{\Omega\Omega}(t,x) &= \frac{1}{2}(1-x^2)\sum_{j=0}^{\infty}t^j\frac{d^2P_j(x)}{dx^2}
\end{aligned}$$

Closed spatial forms

$$
\begin{aligned}
K_{rr}(t,x) &= -\frac{1}{g^3} + \frac{3(1-tx)^2}{g^5} \\
K_{r\Omega}(t,x) &= -\sqrt{1-x^2}\,\frac{3t(1-tx)}{g^5} \\
K_{\Omega\Omega}(t,x) &= \frac{1}{2}(1-x^2)\frac{3t^2}{g^5}
\end{aligned}
$$

where

$$
g = \sqrt{1+t^2-2tx}
$$

Isotropic gradiometric Green's functions

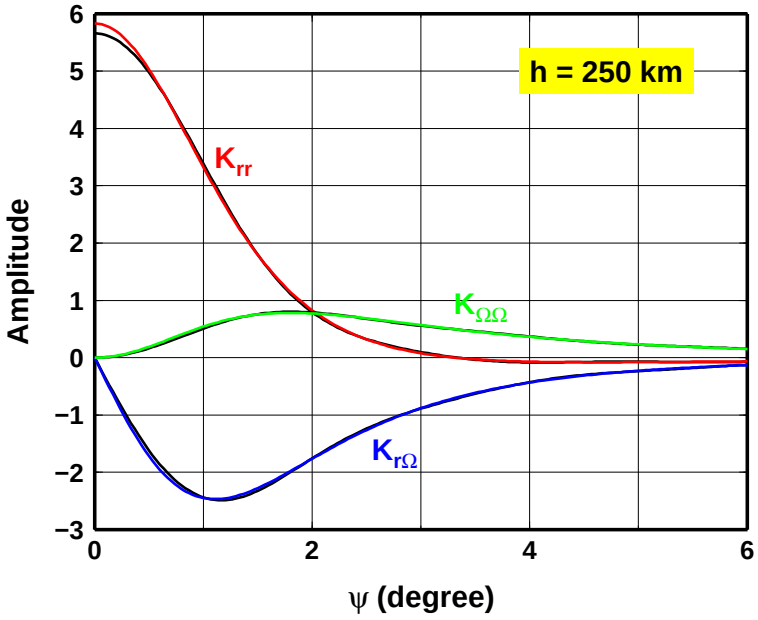

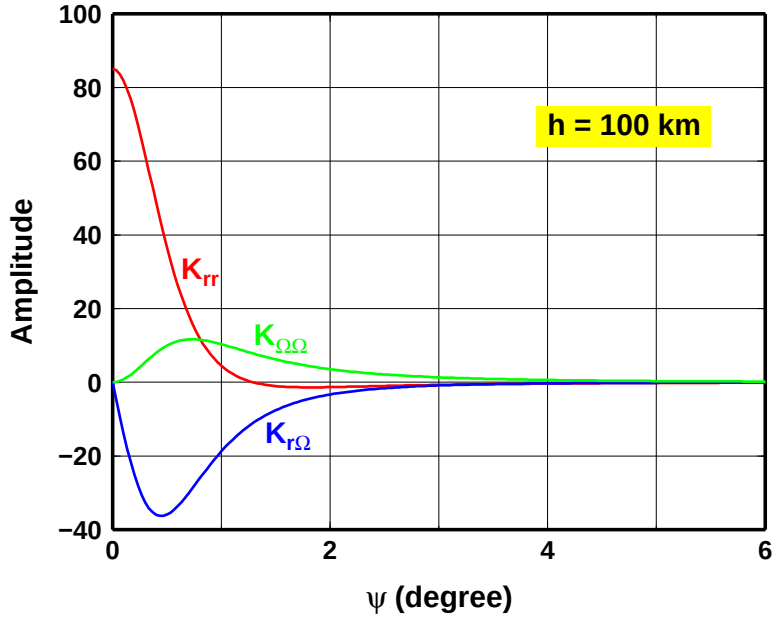

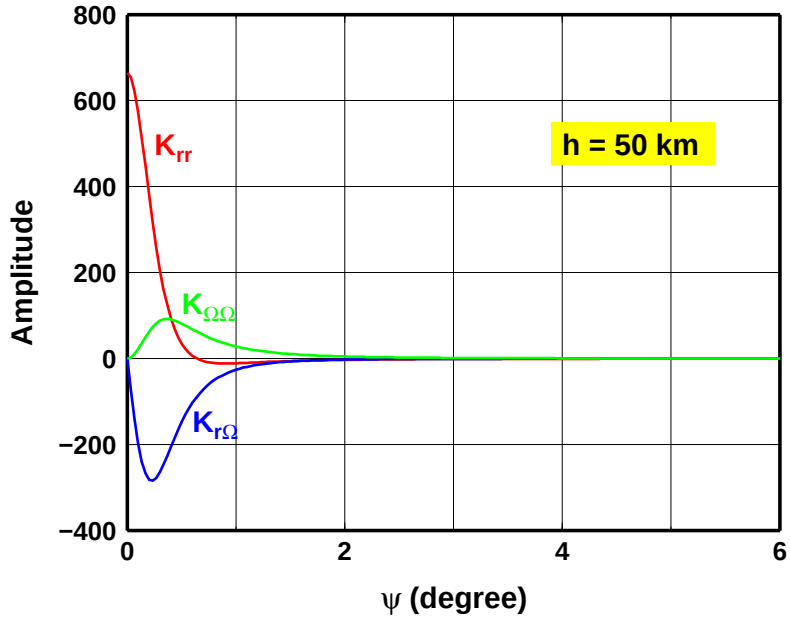

Integral equations for a surface-mass density

For a fixed source position ($r' = const$):

$$\int_{\Omega'} \varrho(\Omega') K_\alpha(\Omega, \Omega') d\Omega' = d_\alpha(\Omega) \qquad \alpha = 1, ..., GOCE$$

The Nyström method discretizes the integral equation by a quadrature rule:

$$\sum_{j=1}^{n} w_j \varrho(\Omega_j) K_\alpha(\Omega_k, \Omega_j) = d_\alpha(\Omega_k) \qquad k = 1, ..., n$$

The Galerkin method:

$$\varrho(\Omega) = \sum_{j=1}^{n} \varrho_j \phi_j(\Omega)$$

$\phi_j(\Omega) \cdots$ a set of n linearly indep. functions (e.g. tapers on a spherical cap)

$$\sum_{j=1}^{n} \varrho_j \int_{\Omega_A} d\Omega \int_{\Omega'_A} d\Omega' \, \phi_k(\Omega) K_\alpha(\Omega, \Omega') \phi_j(\Omega') = \int_{\Omega_A} d_\alpha(\Omega) \phi_k(\Omega) d\Omega \qquad k = 1, ..., n$$

Overdetermined s. of linear algebraic equations for a surface-mass density

$$\boxed{\boldsymbol{A}_\alpha \vec{\varrho} = \vec{d}_\alpha \qquad \alpha = 1, ..., GOCE}$$